AD-A126 264 HETERODYNE DETECTOR/ELECTRONICS DESIGN AND ALIGNMENT OF 1/1
A PULSED CO2 LASE..(U) GENERAL ELECTRIC CO SYRACUSE NY
ELECTRONICS LAB G B JACOBS NOV 82 SCIENTIFIC-2
UNCLASSIFIED AFGL-TR-82-0348 F19628-80-C-0184 F/G 17/5 NL

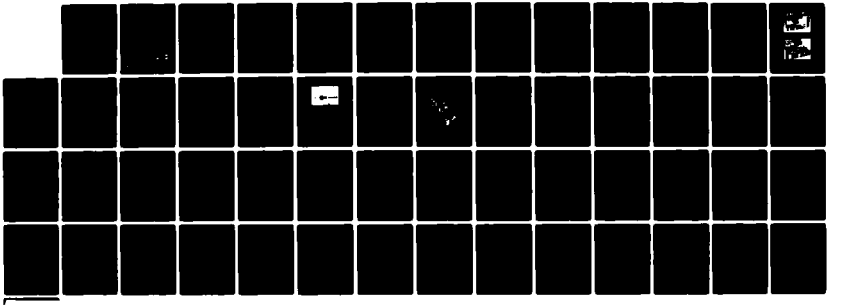

END
DATE FILMED
4-83
DTIC

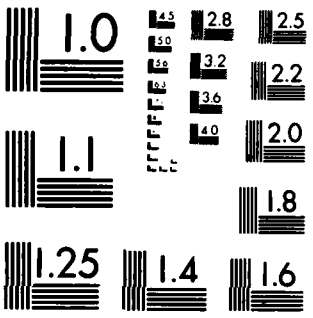

(12)

AD A126264

AFGL-TR-82-0348

HETERODYNE DETECTOR/ELECTRONICS DESIGN AND ALIGNMENT OF A PULSED CO_2 LASER WIND SYSTEM

G. B. Jacobs

General Electric Co.
Electronics Laboratory
Syracuse, New York 13221

Scientific Report No. 2

November 1982

Approved for public release; distribution unlimited

AIR FORCE GEOPHYSICS LABORATORY
AIR FORCE SYSTEMS COMMAND
UNITED STATES AIR FORCE
HANSCOM AFB, MASSACHUSETTS 01731

Unclassified

SECURITY CLASSIFICATION OF THIS PAGE (When Data Entered)

REPORT DOCUMENTATION PAGE		READ INSTRUCTIONS BEFORE COMPLETING FORM
1. REPORT NUMBER AFGL-TR-82-0348	2. GOVT ACCESSION NO. AD-A126 264	3. RECIPIENT'S CATALOG NUMBER
4. TITLE (and Subtitle) HETERODYNE DETECTOR/ELECTRONICS DESIGN AND ALIGNMENT OF A PULSED CO_2 LASER WIND SYSTEM		5. TYPE OF REPORT & PERIOD COVERED Scientific Report No. 2 6. PERFORMING ORG. REPORT NUMBER
7. AUTHOR(s) G.B. Jacobs		8. CONTRACT OR GRANT NUMBER(s) F19628-80-C-0184
9. PERFORMING ORGANIZATION NAME AND ADDRESS General Electric Company Electronics Laboratory Syracuse, New York 13221		10. PROGRAM ELEMENT, PROJECT, TASK AREA & WORK UNIT NUMBERS 62101F 667006BE
11. CONTROLLING OFFICE NAME AND ADDRESS Air Force Geophysics Laboratory Hanscom AFB, Massachusetts 01731 Monitor/Donald R. Fitzgerald/LYR		12. REPORT DATE November 1982 13. NUMBER OF PAGES 54
14. MONITORING AGENCY NAME & ADDRESS(if different from Controlling Office)		15. SECURITY CLASS. (of this report) Unclassified 15a. DECLASSIFICATION/DOWNGRADING SCHEDULE

16. DISTRIBUTION STATEMENT (of this Report)

Approved for public release; distribution unlimited.

17. DISTRIBUTION STATEMENT (of the abstract entered in Block 20, if different from Report)

18. SUPPLEMENTARY NOTES

19. KEY WORDS (Continue on reverse side if necessary and identify by block number)

Heterodyne CO_2 laser
Optical radar
Remote wind shear measurements

20. ABSTRACT (Continue on reverse side if necessary and identify by block number)

Ten-micron heterodyne laser radar offers a new type of remote sensor that can add significantly to our characterization and understanding of the atmosphere. For example, accurate range-resolved measurements of air velocity via the Doppler of aerosol backscatter--to distances of tens of kilometers--will yield a better understanding of wind shear. This report describes the design of the main TEA laser E-beam modulator and of the electronics systems used for AFC stabilization of the laser frequency, and for matching IR detector outputs to the power and Doppler velocity data channels. Practical details are

DD FORM 1 JAN 73 1473 EDITION OF 1 NOV 65 IS OBSOLETE

Unclassified

SECURITY CLASSIFICATION OF THIS PAGE (When Data Entered)

provided for the alignment of the complex optical system used in this laser wind sensor.

TABLE OF CONTENTS

LIST OF FIGURES

LIST OF FIGURES
(Continued)

1 INTRODUCTION

Ten-micron heterodyne laser radar offers a new type of remote sensor that can add significantly to our characterization and understanding of the atmosphere. For example, accurate range-resolved measurements of air velocity via the Doppler of aerosol backscatter--to distances of tens of kilometers--will yield a better understanding of wind shear. This report describes the design of the operational laser radar trailer facility to be built by General Electric for the Air Force Geophysics Laboratory (AFGL) under Contract F19628-80-C-0184.

As noted in our proposal, Pulsed Heterodyne CO_2 Laser/Scanner System, dated April 1980, the system is to incorporate the high pulse repetition frequency (PRF), high-power electron-beam injection CO_2 laser developed earlier by the General Electric Company. The system is to be assembled in a trailer to be supplied by the government and will permit hemispherical scanning with a laser beam of less than 2×10^{-3} degrees beamwidth.

This 2nd scientific report is a design evaluation report, as was the first. This report contains most of the design descriptions of the first plus additions and/or corrections that bring it up to date. The chief additions are in Section IV. In particular the recent work on the electronics, Section H and Heterodyne Techniques, Section I, have been added.

This report is intended to aid the government in judging the capability of our design to meet the government's requirements. For the purpose of convenience, we list in Exhibit A, the contract specifications that our design is to meet. To date, we have set up a breadboard of the heterodyne laser radar facility and have tested the critical techniques to be used. In addition, we have completed the engineering design and shop work in three major areas of construction (laser, scanner, and optics). The electronics design is essentially completed and wire shop work well underway.

As discussed below all the equipment has been collected in our penthouse laboratory and is being assembled for subsystem and system tests.

EXHIBIT A

Attachment 2
Engineering Description for a Pulsed Heterodyne CO_2 Laser/Scanner System (Full Hemispheric Scanning)

1.0 Introduction

1.1 This specification describes requirements for the development of a moderately high energy, high prf, pulsed doppler CO_2 laser/scanner system. The system will be used for experimental studies in remote sensing of atmospheric wind patterns and aircraft wake vortices. The system will operate on the principle of heterodyne detection of the frequency shifted signal received from atmospheric particulate backscatter. A nominal range of 20 km is the design goal with a minimum range of approximately 1 km.

1.2 System power levels, frequency stability, optical configuration, and sensitivity shall be such as to provide a radial wind measurement over the velocity range of ±50 meters/sec full scale. Transmitted signal pulse length shall be selectable to provide a 2 meter/sec velocity resolution at long pulse and a 5 meter/sec resolution at short pulse.

1.3 The laser beam shall scan in azimuth and elevation under remote operator control.

2.0 Specifications

2.1 The laser shall produce plateaus of 5 microsecond pulse duration at a 1-Joule energy level and of 1 microsecond pulse duration at an 0.2-Joule energy level. The energy shall be single wavelength, single transverse mode, and single longitudinal mode.

2.2 The gain switch spike to plateau ratio shall be reduced to a practical minimum, and not to exceed 3 to 1.

2.3 Provisions for control of radio frequency interference and acoustical noise shall be included in the design.

2.4 The pulse repetition frequency shall be 50 pps or greater for automatic frequency control (AFC) and to permit data signal averaging for enhanced signal to noise ratio.

2.5 The system shall provide separate intermediate frequency (IF) amplifier/discriminator channels for optical system AFC loops and as a data output discriminator to interface with existing government-owned signal processing and display systems. The data IF/discriminator shall provide a 70 MHz center frequency with linear bandwidth sufficient to provide ±50 m/sec full scale radial wind speed data with a resolution of 1 m/sec at a 5 microsecond pulse duration and a resolution of 5 m/sec at a 1 microsecond pulse duration.

2.6 Frequency chirp during the pulse shall be controlled to 0.2 MHz p-p, for compatibility with requirement 2.5

EXHIBIT A

2.7 The receiver infrared (IR) detector shall be a wideband (Hg, Cd, Te) unit cooled with a liquid nitrogen dewar of at least four hour hold time. Alternate cooling methods of equivalent performance may be proposed. Detectivity of at least $D^* = 5 \times 10^9$ cm Hz 1/2/w and a quantum efficiency of at least 40% shall be provided. Additional pyroelectric or other IR detectors shall be incorporated as needed for AFC control and for establishing and monitoring system alignment and performance. Means shall be provided for continuous wideband monitoring of the transmitted signal waveform and power level. Efforts shall be made to provide optimum phase matching of the signal and local oscillator beams and sufficient stable local oscillator power to maximize the system heterodyne detection efficiency.

2.8 The laser small-optics configuration will be mounted on a suitable optical bench for contractor installation in a government-furnished trailer located at the AFGL Weather Radar Facility, Sudbury, MA. An 8 foot by 32 foot equipment trailer has been requested for use with this system. Mechanical modifications of the trailer will be provided by the government in accordance with acceptable contractor specified requirements for system housing and stability. Of the space available, no more than 8 feet × 24 feet shall be required for the laser system. Provision shall be made for necessary equipment access for alignment and maintenance within this space. Prime power (3ϕ and 1ϕ) and water for heat exchanger cooling will be provided by the government.

2.9 The laser system shall meet the requirements of these specifications over an ambient temperature range from 18°C (64°F) to 24°C (75°F).

2.10 The optical system shall include a beam-expander telescope of approximately 30 cm diameter and the necessary components and mounts to provide azimuth and elevation scan capability. An overall optical system efficiency of at least 10% is required. It is necessary that the scanner be capable of operation roof mounted on top of the trailer.

2.10.1 The scanner shall provide full hemispheric elevation over azimuth beam pointing under remote servo loop or stepping motor control.

2.10.2 The contractor will provide remote positioning controls, azimuth and elevation indicators, and data readout electrical signals for installation in the trailer. Angle resolution and repeatability for this application shall be 0.25 deg or better. Holding stability of 1 milliradian or better is expected for 10 knot winds. A scanning rate selectable up to two rpm is desired. A practicable degree of adverse weather protection shall be provided for the external optical system.

2.10.3 Optical components shall be included in the system suitable for visual examination of targets and checking of system alignment.

2.11 The system design shall attempt to minimize the required fresh gas mixture make-up rate.

2 SYSTEM DESIGN AND PLANNING

The present system embraces a wide variety of engineering technologies and incorporates a large proportion of narrowly specified purchased components. The single, simplest format for categorizing, scheduling, and integrating the engineering, construction, specification, and purchasing of the various components is suggested by the functional block diagram of the system. Thus the four main subjects of the following discussion are TEA laser, scanner, small optics and electronics.

Figure 1 shows a basic diagram of the system and the key components that make it up. The upper right block, "TEA Laser/Modulator," provides the transmitter pulse of the required power and timing to the "Telescope/Scanner," which forms it into the required beamwidth, transmits it in the required direction, and delivers the returning target echo to the heterodyne receiver, which is located in the "Electronics" subsystem. The "Small Optics" generates the coherent, local, optical beams necessary both to control the transmitter wavelength and to heterodyne the weak target echo up to a more useful power level at the intermediate frequency (IF) of the receiver. The scanner's position control system and the electronics of the receiver's IF must be compatible with the customer's computer position commands and computer data processing, respectively.

Many technologies--optical, electronic, and control--are employed in these subsystems, and all must be carefully designed to permit the required system performance. Yet certain areas must necessarily receive the most attention, either because they are new and not well developed, or because they are critical to overall system performance.

In the TEA laser section, the most attention is being placed on the 120 kv, 15 ampere, 10 μs modulator that provides the laser's electron-beam pulse. In the scanner area, the diffraction-limited 12-inch-diameter Dall-Kirkham Telescope and the digital control of azimuth and elevation position are most important. In the small optics subsystem, the key problem has been to provide stable automatic frequency control of the three lasers.

General Electric is also supplying information and suggestions to aid in the government's design of the government-furnished equipment (GFE) trailer. In this area, the scanner elevator and the road-travel isolation system are most important. The government is also providing the data processing system by which Doppler versus range data are extracted from the receiver's IF. In this area, the problem of pulse-to-pulse frequency jitter and, of course, the statistical treatment of the huge amount of data will be most important.

Figure 2 shows the penthouse test installation now in progress. On the right, in the upper view, are the three control racks. The scanner, to be mounted later on the trailer roof, is shown on its temporary 2 × 4 scaffolding. None of the mirrors, lens or other delicate optical components are shown. These will be installed shortly, after rough work of plumbing,

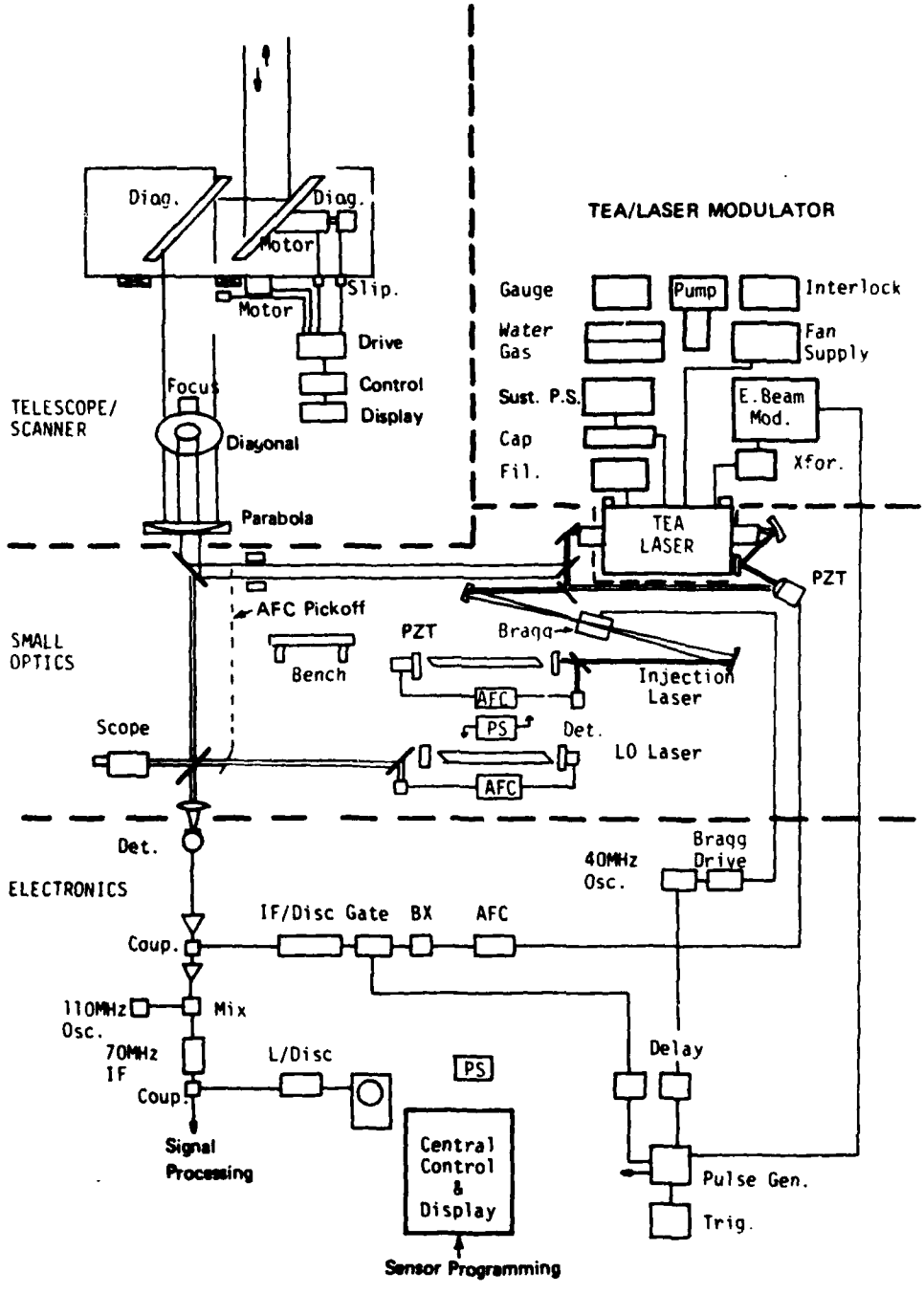

Figure 1. Demonstration System with Separate LO Laser

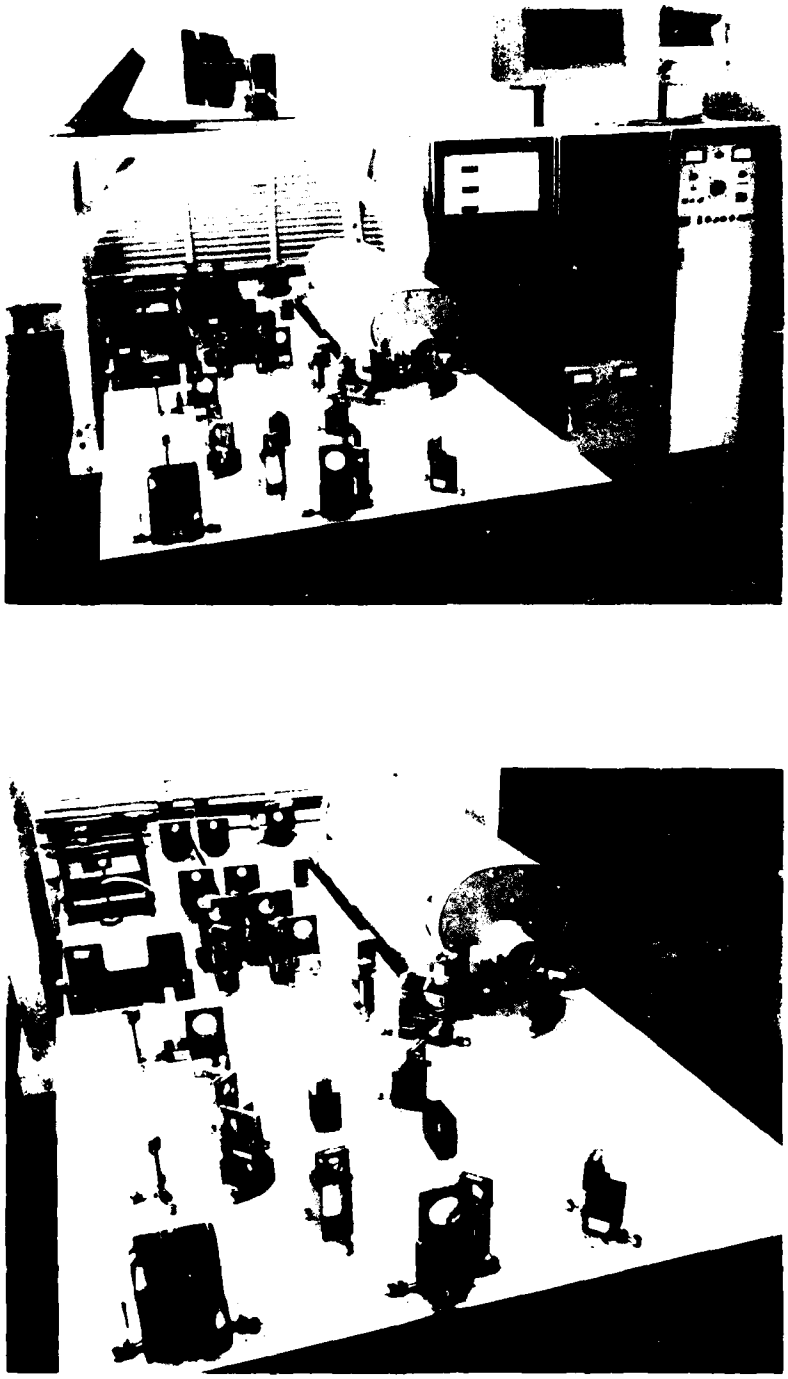

Figure 2. Penthouse System Test, Partial Installation

cabling, vacuum lines and electronic chassis are completed. The blinds on the window hide the view looking south over the city of Syracuse and into the hills about 20 km away. The clearance and target terrain is excellent for observation of both standard targets on the ground and atmospheric effects at all attitudes although high zenith angles will be restricted unless we put a hole in the roof.

The lower view shows nearly all the optical mounts required to manipulate the laser beams. The 12" Cassegrain telescope mirrors will rest in the mounts on the subdeck on the left (see Figure 8). The LO and injection laser tubes (see Figure 13) will rest in the supports in the upper center. To repair or modify the TEA laser its top flips up and back without touching any of the optical mounts in the rest of the system. The electron gun of the TEA laser, its vacuum system and the high voltage pulses are under the TEA laser, on the right. (See Figure 7).

3 SYSTEM DESIGN

3.1 INTRODUCTION

Figure 3 shows the initial system design contemplated early in the program. Figure 1 shows the final system evolved during the design effort and successfully demonstrated as a breadboard in the GE TEA laser facility. In this section we discuss the factors governing this evolution.

3.2 AFC

The system shown in Figure 3 has the advantage of simplicity. The same low pressure laser provides the source of both local oscillator and injection light, and only two AFC loops are needed, one on the reference laser and one on the TEA laser. It was recognized early on that spurious feedback from the TEA laser into the detector (shown in Figure 6) could cause noise in both AFC loops and even endanger the detector. But this feedback was to be eliminated by pulsing the modulator off about 1 μs before the TEA laser power came to a maximum.

When this system was set up, it was found to be unreliable. The lack of reliability stemmed, first, from the large time jitter of the TEA laser pulse, which is itself a function of the injection signal frequency, second, from time jitter during manual adjustment of the trigger delay, and, third, from the AFC noise generated by feedback leaking through even the properly timed Bragg cell.

As a result of breadboard tests performed on this contract, the system of Figure 1 was subsequently set up. With this configuration, separate low pressure lasers provide the LO and injection signal, but both are dithered to line enter by their own dithering AFC systems. To avoid the instantaneous frequency errors due to dither, the two low pressure laser AFC systems use the same dither reference frequency. The dither reference signal is also used to dither the TEA laser cavity. This is accomplished with a trio of amplitude and phase controls used to synchronize the frequency shifts of the three. This system was found to work well, since it held the maximum instantaneous differences owing to all effects to less than about 1 MHz.

A third AFC technique was contemplated that we had used very successfully on a BMD contract in 1978. In this scheme, only one of the LO pressure lasers is dither-stabilized. The other is made to lock to the first by a heterodyne AFC system. The only objection to this design is that it requires an additional Bragg modulator (or other EO switch) and an additional cryogenic detector. This system is a good backup in the event the dither stabilization is not sufficiently stable in the presence of large variations in room temperature. (Temperature-induced mechanical misalignment of the low pressure laser cavities can cause frequency shift from line center due to frequency pulling of the cavity grating.)

3.3 IF

In Figure 1 the injection signal is offset by 40 MHz to provide, ultimately, a 40 MHz intermediate frequency at the output of the detector.

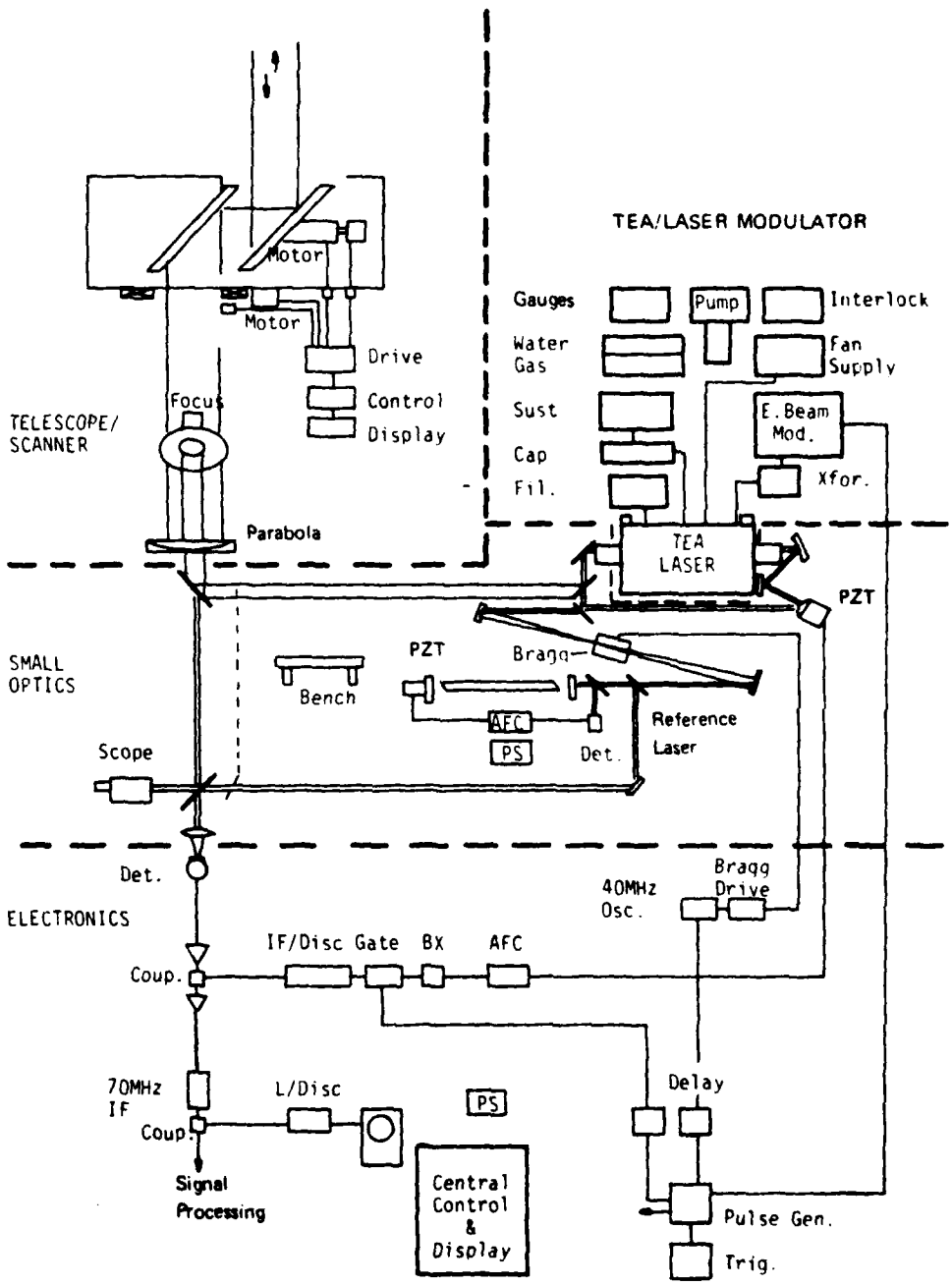

Figure 3. Initial System

An electronic local oscillator (LO) of 110 MHz provides an IF of 70 MHz for the wideband IF amplifier immediately preceding the signal processor. The selection of 40/70 MHz dual IF rather than a single 70 MHz IF was based on the need to maximize the power injected into the TEA laser. A Bragg modulator at 40 MHz will provide more than twice as much energy in the first order as a 70 MHz unit, at the present state-of-the-art. The amount of injected energy required to control the longitudinal modes and transitional wavelength of a TEA laser is a function of the precision with which the AFC systems can control the instantaneous frequency of the TEA laser cavity and the injected frequency. In general, state-of-the-art AFC systems require about 1 watt of injected power, but the more the power, the more reliable the control system and the less jitter in TEA laser's amplitude and pulse time.

3.4 DUPLEXER TESTS

Design of the basic radar system raised another key problem. The use of coaxial transmit and receive beams (rather than side-by-side beams) is necessary for practical hemispherical scan but causes problems due to local backscatter of some of the transmitted power into the receiver detector. We discuss the design of a low back-scatter duplexer (T-R switch) in the small optics section, but since the calculation of spurious back-scatter is only approximate, at best, it was important to make at least some tests before the system design was fixed.

Using an eight-inch diameter receiver parabola and a two-inch diameter transmitter beamwidth, we simulated some of the backscatter problems of a coaxial system using the optical system shown in Figure 4. Note that very high power TEA laser energy falling on the edges of the 2-inch diagonal and backscattered from those edges or from dust on the roof top scanner will be collected by the 8-inch parabola and directed toward the receiver detector. Detector damage will occur if only 10^{-9} of the transmitted energy falls on the detector. Figure 5 shows a photo of the receiver output display of the system presented in Figure 1 operating as a radar on remote targets and using the telescope and duplexer optics of Figure 4. Measurements showed that the spurious backscatter from the optics was about the same magnitude as the intentional AFC reference pickoff, and neither was greatly larger than a typical signal such as that from a water tower at one mile. TEA laser peak power was about one megawatt. It is interesting to note that Figure 5 also shows the aerosol return from the transmitter site out to the tower. Beyond the tower, the aerosols are in a shadow. For these tests the transmitter and receiver beamwidths are not matched, and thus, the aerosol return is rather weak. But the tests do show the form of the signal for this type of target. For example, the apparent modulation of the aerosol return is due to the random interference (or speckle) in the diffuse aerosol scatter as well as to spatial modulation of the aerosol density.

The breadboard system tests also demonstrate that we have learned to control the major sources of RF interference and the major sources of frequency instability in the laser AFC.

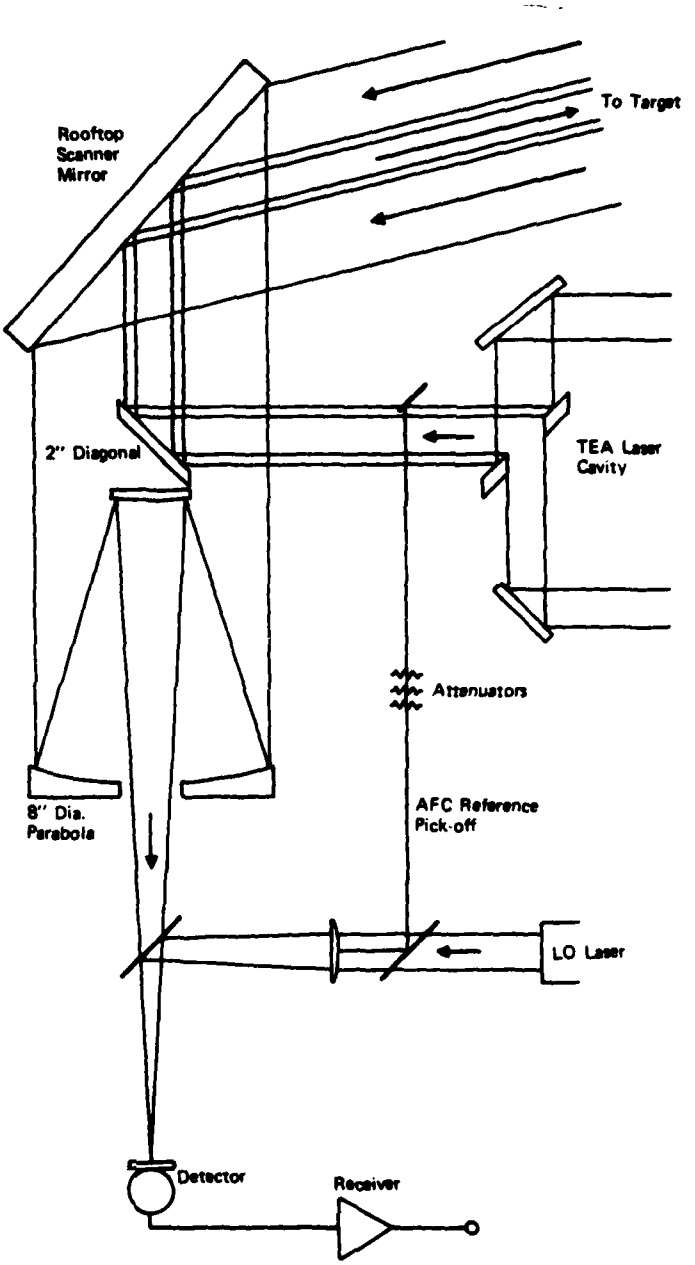

Figure 4. Breadboard 8-inch Optics

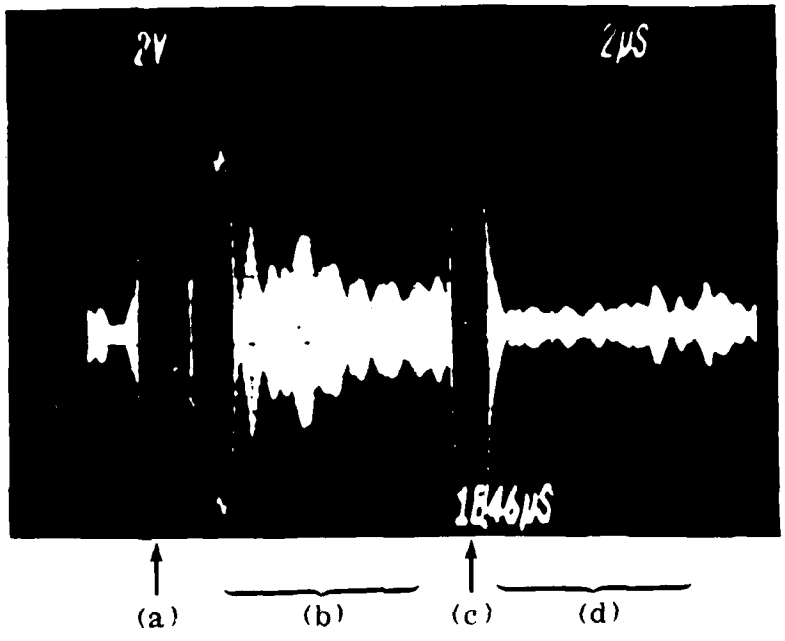

(a) AFC pickoff plus local mirror backscatter
(b) Aerosol return
(c) Water tower at one mile
(d) Shadow in aerosol return behind tower

Figure 5. Typical Single Pulse Target Signature at Receiver IF Output

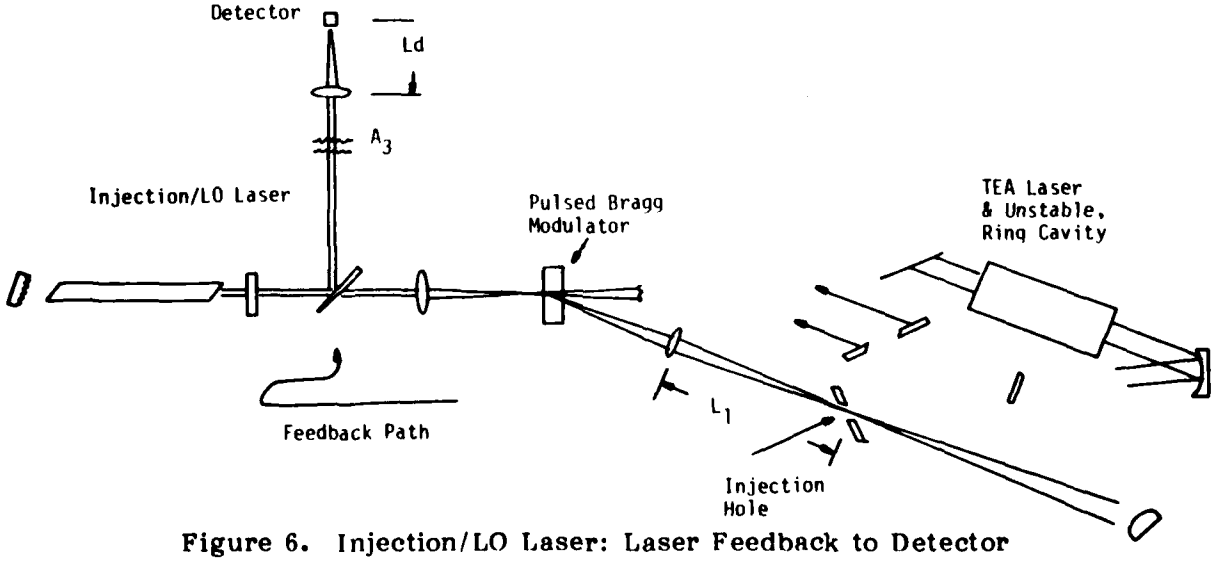

Figure 6. Injection/LO Laser: Laser Feedback to Detector

4 SUBSYSTEM DESIGN

4.1 INTRODUCTION

In this section, we examine the designs of the several subsystems and the analyses, tradeoffs, and comparisons that led to their selections.

4.2 TEA LASER/MODULATOR

The electron beam injection CO_2 TEA laser, shown in Figure 7, is the heart of the high-power heterodyne laser radar. The reason the electron-beam injection technique is used is to achieve the long pulse length and low frequency chirp necessary for 1 meter per second (200 kHz) doppler resolution. The usual ultraviolet preionized TEA laser has pulse lengths that are limited to one or two microseconds and may have a chirp of several megaHertz.

The TEA laser being built for AFGL is the same as the one built by General Electric for its heterodyne laser radar facility. It was originally designed for pulse energy of 5 joules and pulse repetition rates of 300 pulses per second (PPS). The new unit, for example, retains the 40 kW heat exchanger because this was less expensive than designing a new one. Thus, if in the future it becomes desirable to have higher power or higher pulse repetition rates, the system can be expanded easily.

Several improvements over the construction shown in Figure 7 will be incorporated in the new model. First, the TEA laser windows (items 37 and 39, Figure 8) have been converted to nearly perpendicular NACL flats rather than Brewster windows to give better beam quality and power handling capability. Second, the foil support plate has been redesigned to provide longer foil life by the avoidance of thermal expansion gaps previously thought necessary. Third, some increase in filament diameter will be incorporated to improve filament life. And finally, the CO_2 circulation fans are now 60 Hz, which avoids the need for a 400 Hz power supply. Because three-inch diameter diffusion pumps are no longer the industry standard, we have changed to one four-inch diffusion pump and one, correspondingly larger, fore pump.

Figure 1 shows the various peripherals, premixed makeup gas, vacuum gauges, vacuum and water interlocks, sustainer power supply (5 kW, 20 kV), and sustainer capacitor (14 μF, 25 kV). The latter is located directly under the laser to reduce RF interference and sustainer pulse rise time.

The TEA laser is well shielded with lead to protect the operators from X radiation and is mounted directly on the main optical bench to maintain alignment with the optics. (See Figure 9.) The steel honeycomb optical bench has been custom designed to hold the heavy weight and to allow access to the high voltage bushings below.

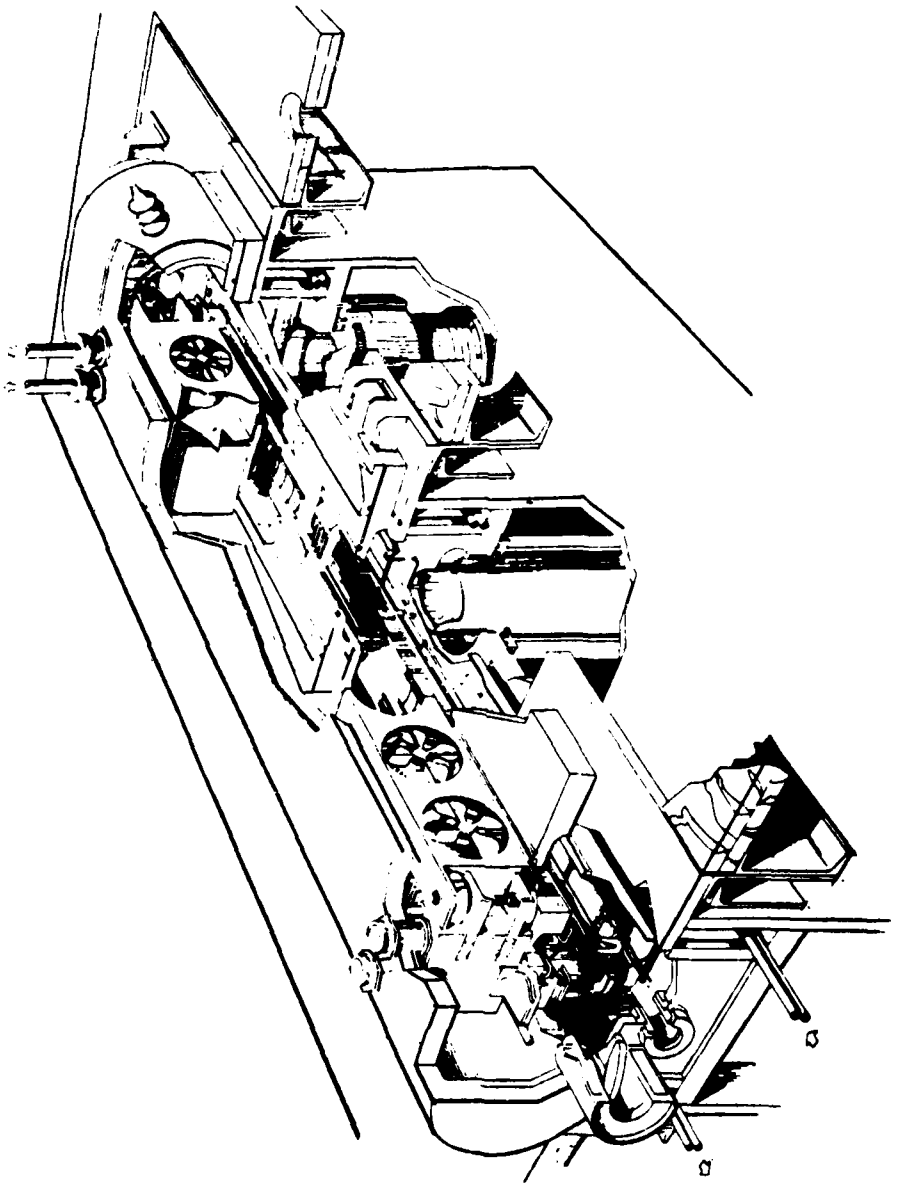

Figure 7. EBI/TFA Laser

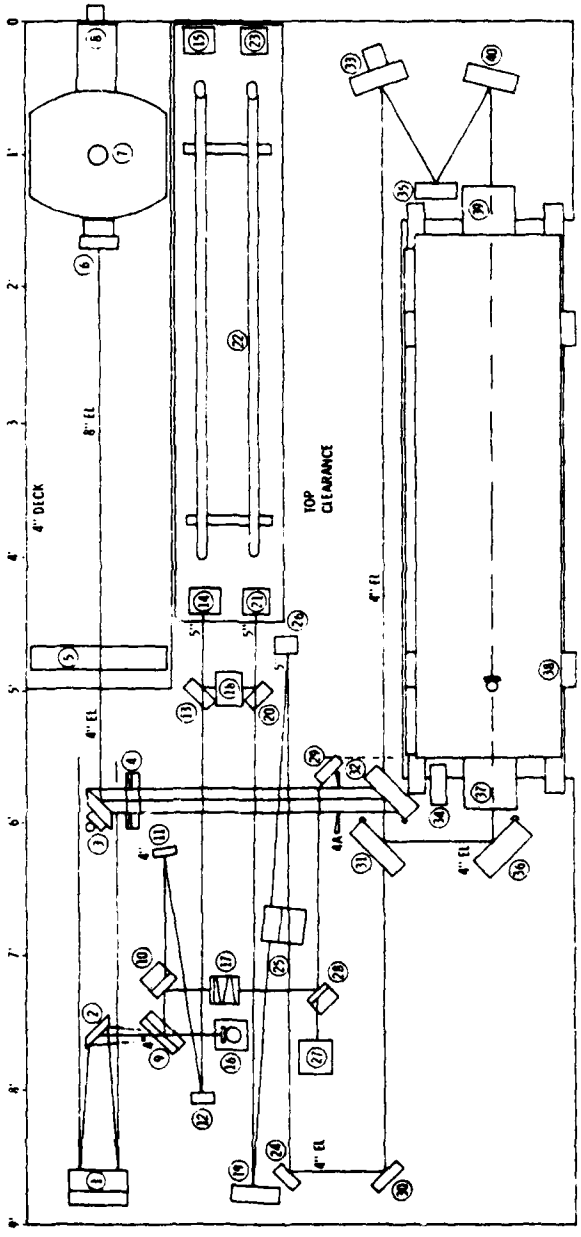

Figure 8. Small Optics

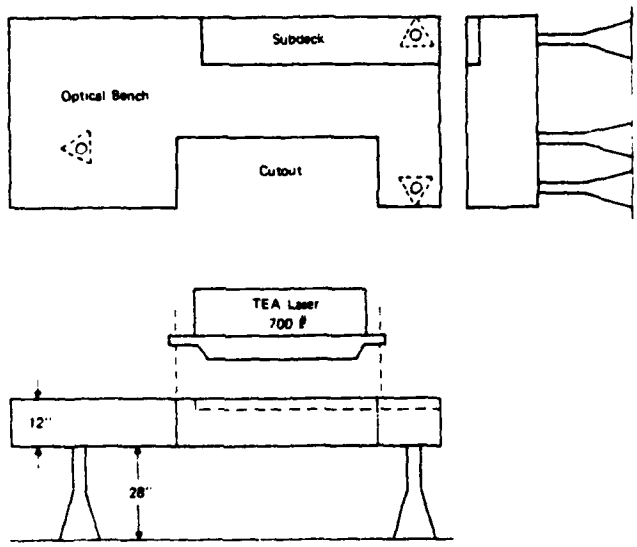

Figure 9. Optical Bench

The electron beam modulator is to deliver 120 kV, 15 ampere pulses of either 10 μs or 5 μs to the electron gun at up to 50 PPS. With an additional modulator rise and fall time of about 1 μs each, the laser itself will deliver either 5 μs or 1 μs light pulses. Figure 10 shows the schematic of the electron beam modulator. The modulator uses a hydrogen thyraton (V1) and a pulse forming network to deliver a 20 kV, 100 ampere pulse to the high-voltage output transformer (T1).

Figure 11 shows a cut-away side view of the modulator, which will be located under the optical bench and connected directly to the laser's electron gun. Note that all of the modulator except the 2.5 kW, 25 kV DC power supply is located in one box under the laser, thus minimizing RF interference and safety problems. The high voltage section, including the pulse transformer, pulse forming network (PFN), resonant charging inductor, and main thyratron are located in oil in the lower section. The low voltage sections including the drive amplifiers and their power supplies are located in air above the oil box. The modulator will be bolted to a 4 foot × 9 foot reinforced trailer bed support plate through stiff vibration isolators.

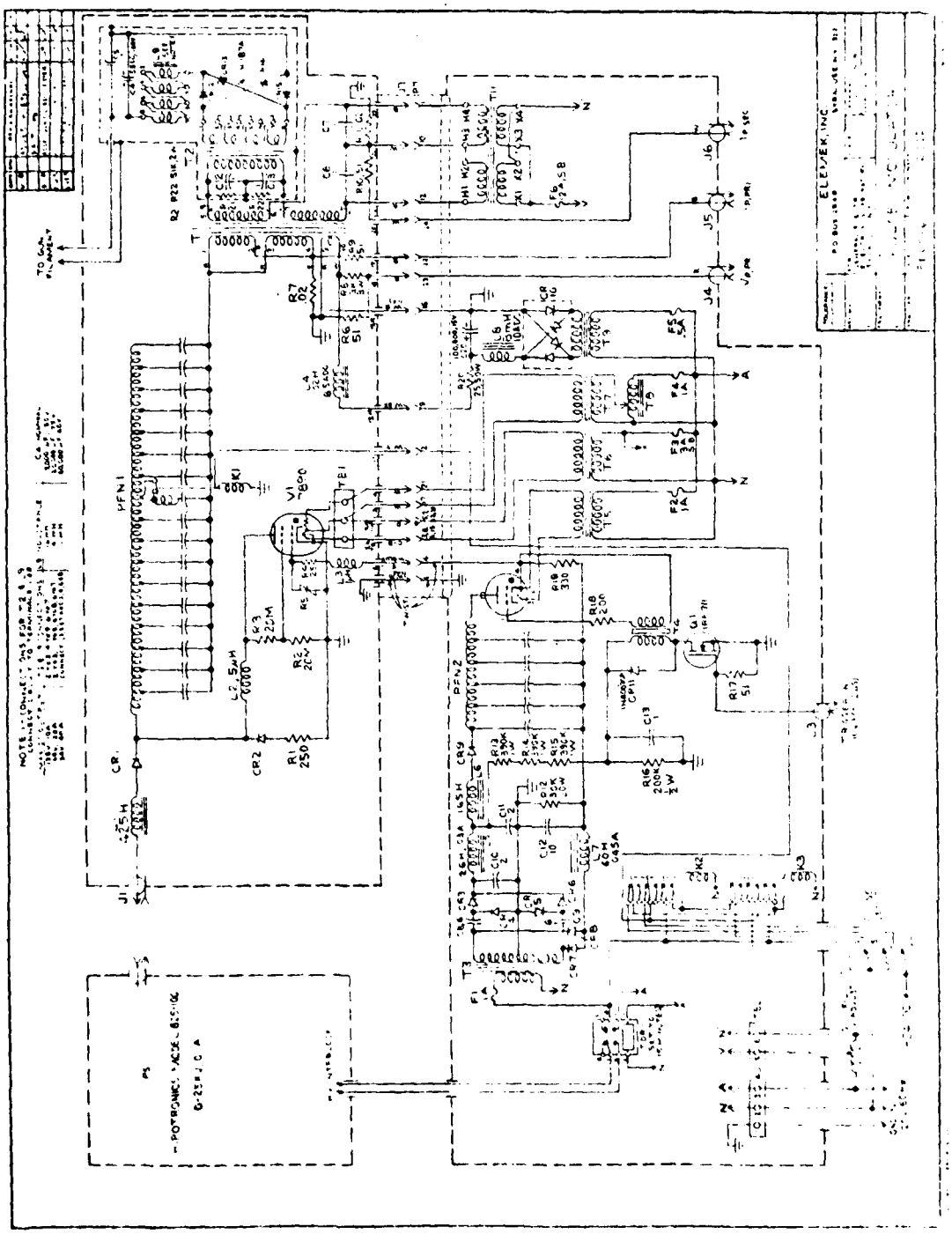

Figure 10. Electron Beam Modulator

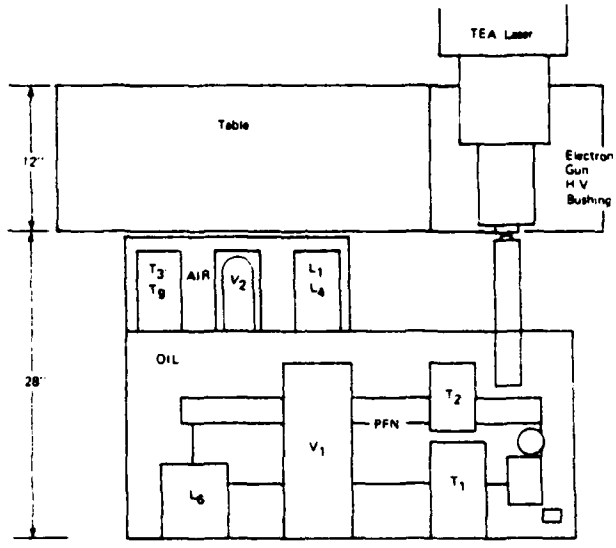

Figure 11. Electron Beam Modulator Layout

Although the PFN/thyratron modulator technique has the disadvantage of requiring a rather large step up (6:1) in the pulse transformer; compared to a hard tube modulator, it has the advantage of small size. The 6:1 step-up, with its large leakage reactance, causes, in our case, a 1.1 μs rise time and a 2 μs fall time (to 10%). However, since the electron-beam does not penetrate the foil below an electron energy of about 80 kV, the electron density pulse length, into the laser gas, has a much faster rise and fall time.

The modulator pulse output voltage will be controlled by a Variac on the panel of the control box located in the three-rack control panel next to the optical bench. This unit also supplies overload protection, interlock switching, and voltage/current monitors. The 2.5 kW 25 KV DC supply itself will be in an oil filled container under the optical bench. The pulse current is controlled by the filament current to the emission-limited filament of the electron gun.

The high voltage pulse transformer is quite small, using a single "C" core 9 inches × 5-1/2 inches × 1-1/2 inch. Each leg of the core has an 82-turn, single-layer primary of #17 wire under a 6-layer secondary of 492 turns. The primaries are connected in parallel. The secondaries, effectively in parallel, provide a bifilar filament supply winding capable of 480 volts, 2 amperes, 60 Hz to T_2. This design allows unusually

small secondary wire size (for 1 kW of filament power) and, thus, reduced secondary distributed capacity because of this and the match between volts per layer of the primary and secondary. Winding margins of 1 inch plus 1/4 inch polystyrene end plates will provide adequate breakdown voltage. Interwinding insulation will take advantage of the high skin-effect dielectric strength of mylar (one-quarter-mil-thick mylar has a voltage breakdown of 19000 V/mil).

The resulting close spacing between layers, of course, will minimize leakage reactance. A DC reset winding will be incorporated in the transformer to increase the effective pulse flux change. This winding will also serve as a voltage monitor. Secondary and primary pulse current will be monitored by low-inductance current shunts, as is shown in Figure 10. Total leakage reactance and distributed capacity referenced to the primary are 93.1 μH and 3705 pF respectively.

Because of the relatively high transformer input impedance, the PFN impedance must be relatively high, which results in non-standard PFN capacitors (.0014 μF per section at 45 kV). Seventeen sections of line will be used. Each inductor will be 32 turns of #17 wire 3.13 inches long and 2.4 inches in diameter. As is shown in Figures 11 and 12, the two 5 μs PFN coils are at right angles to each other to remove mutual inductance effects. The relay, K1, in oil, will be remotely controlled when the operator wants to change laser pulse length.

Figure 10 shows the control connector among the several units of the modulator. For example on the center rack of Figure 22 is the switch to change the laser pulse length from one to five miroseconds via relay K1. This is a vacuum relay to standoff in 40 kV PFN charge. However since the relay could not handle the energy involved it should not be changed while the power is on. The logic of interlock relays K_2 and K_3 is arranged to prevent this.

Because of the high primary impedance (200 Ω), the resonant charging inductor must be of unusually high reactance: 425 henries. A relatively small pair of cores of 1-5/8 inch × 4-3/16 inch window, having 84 layers and 255 turns per layer, is required. A charging diode (CR1) will be used to hold the line at twice the DC charging voltage of 40 kV regardless of the pulse repetition frequency. The pulsed tube is an ITT Hydrogen Thyratron; Type 7890, rated at 2400 A and 40 kV. It uses a 200 watt filament and a 35 watt heater. With a bias of -650 volts, the tube requires about 1200 volts grid drive. This is achieved by a 4635 thyratron rated at 90 A and 8 kV. This drive thyratron uses a 1 μs PFN to provide a long enough drive pulse to allow the 7890 to become fully conducting. Driving the smaller thyratron is an IRF 333 power metal-oxide-semiconductor field-effect transistor (MOSFET) with an output of 1 ampere and gain of 20 dB. The 10 volt 50 Ω master trigger pulse (see Figure 1) will be sufficient to drive this MOSFET stage directly.

The charging diode (CR1) and reverse swing diode (CR2) are Semtech, potted, high-voltage, silicon-diode stacks.

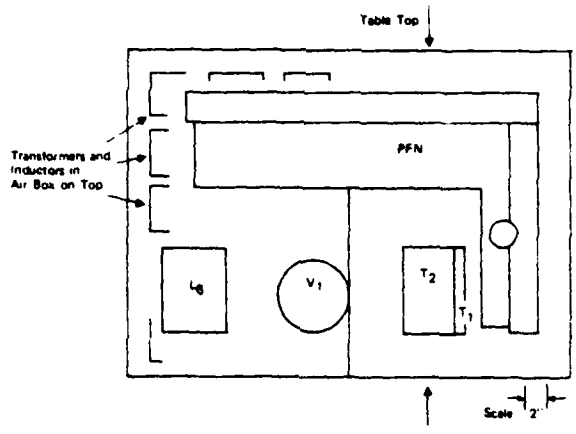

Figure 12. Electron Beam Modulator Layout: Top View

4.3 SMALL OPTICS

In this section, we will describe the function and layout of the optical bench and then return, in Sections 4.4 and 4.5, to discuss details of the major selections evident in this system, namely the Dall-Kirkham telescope optics and the opaque beam-splitter type duplexer.

The small optics are laid out on the optical bench (Figure 9), which is 4 feet × 9 feet pretapped stainless steel honeycomb 12 inches thick. A 16 inch × 50 inch cutout on one side holds the 700# TEA laser. A 60 inch × 13 inch subdeck holds the 12-inch diameter telescope and 12 inch × 17 inch first output mirror down to a level convenient for aligning it with the rest of the system. The table weighs about 2 tons altogether. It is held by three legs bolted directly to a 4 foot × 9 foot reinforced trailer deck, which is described further in the "trailer" section. The 4 foot × 9 foot × 28 inch volume under the bench is used for the high-voltage electron beam modulator, the vacuum pumps, and the terminals for the several sources of water, gas, and power also discussed later. The 12-inch × 17 inch output mirror sends the main laser beam straight up into the scanner mounted on the trailer's roof. The location of the bench must allow exact alignment of the output beam and the scanner.

Figure 8 shows the layout of the small optics system. The TEA laser, 38, is mounted on stiff vibration-isolator pads in the 16-inch × 50-inch cutout. It regeneratively amplifies the laser power from the injection laser around the TEA laser cavity consisting of mirrors 31, 32, 33, 35, 40, and 36. These constitute an unstable, confocal, positive branch ring cavity

whose design is intended to optimize the laser power, pulse length, and spectral and spatial beam coherence. Much of the design work is reported on in an earlier contract[1]. The wavelength of emission is determined by the injection signal's wavelength. Thus, no grating is required in the cavity. The effective Fresnel number is selected to favor the lowest order transverse mode. The resulting longitudinal mode is that closest to the injection frequency. The output beam is annular, 40 mm OD and 30 mm ID.

The magnification of the unstable cavity is controlled by convex mirror, 33, and concave mirror, 40, of radii-298 cm and +400 cm respectively. All cavity mirrors are 99% reflective Kanagen/copper.

The two low-pressure flowing-gas CO_2 lasers, 27, (see Figure 13) supply the local oscillator signal and the injection signal. Commercial sealed lasers have very limited life time (<1 year) and commercial flowing gas units are not sufficiently stable for heterodyne detection. Thus, General Electric has elected to build rather than buy these units. The injection laser uses a Littrow grating, 23, and an 85% coupling mirror, 21. The mirror, 21, is supported by a piezoelectric transducer that adjusts the laser's wavelength exactly to P-20 line center. The injection laser output is focused on the 40 MHz Bragg modulator, 25, by spherical mirror, 19, and then refocused to about 3 mm diameter to enter the TEA laser cavity mirror, 31. Item 31 has a 4 mm diameter hole to accommodate this injection.

The TEA laser output is collected by a 40 mm ID scraper mirror and directed to the telescope via copper diagonal mirror 3. To minimize the TEA laser energy illuminating the edges of this diagonal, and thus getting back into the cryogenic detector, 16, we use two sharp-edged graphite shrouds, 4 and 4a, 41 mm in diameter. If the beam is misaligned, the graphite lights up and thus provides the operator with a continuous alignment check. Item 34 is a solid graphite block that captures any counterclockwise cavity power and lights up to tell the operator that injection power is inadequate.

The TEA laser output, which is collimated, next illuminates the spherical convex Kanagen/copper secondary of the Dall-Kirkham (sphere-ellipse) telescope and is expanded to illuminate the 12-inch diameter objective. The transmit beam, now expanded from 40 mm to 160 mm diameter, next illuminates the 12-inch × 17 inch diagonal mirror, 7. The beam then goes straight up into the 12-1/2 inch diameter throat of the scanner located on the trailer's roof. Diagonal 7 has a 2-1/2 inch perforation that enables the operator's boresight telescope, 8, to be collimated coaxially inside the transmit beam. Since the laser beam is already an annulus, no power is lost in the "beamsplitter" itself.

Laser power reflected back into the receiver from such sources as the rod supporting the secondary may damage the detector and is the subject of Section 4.4. Since the laser beam is an annulus no power illuminates the

---

[1]Investigation of Efficient High Power Coherent Laser-Generated Pulse Burst Waveform, G.B. Jacobs, L. Snowman, and F. Shapiro, BMD contract number DASG 60-77-C-0141, December 31, 1978.

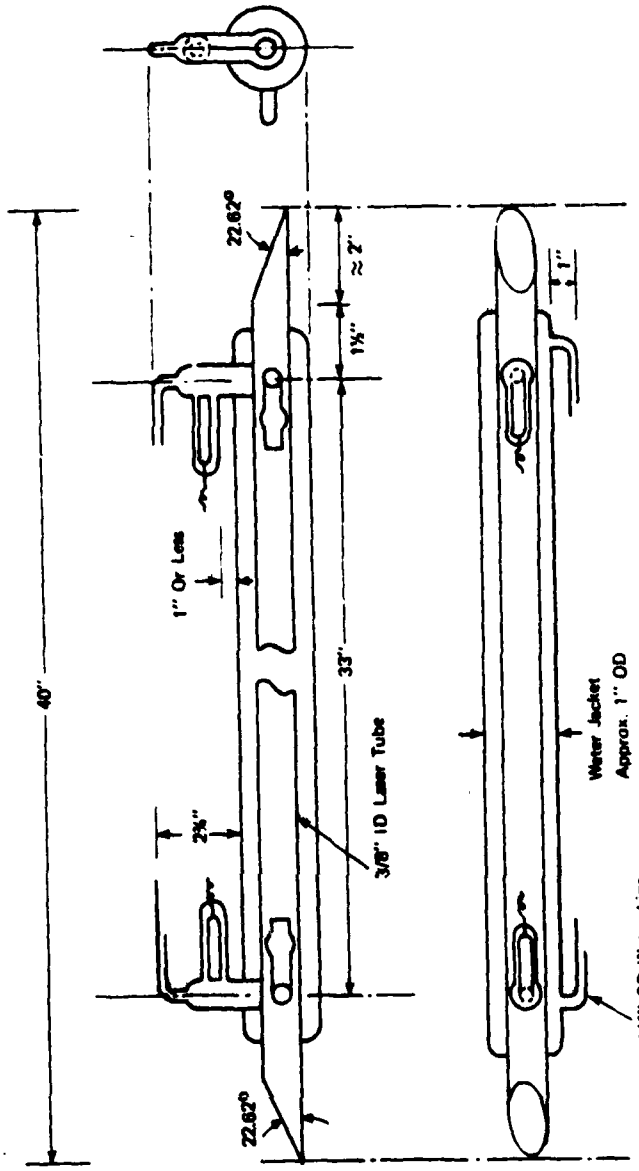

Figure 13. Flowing Gas LO/Injection Laser Tube

first Fresnel zone at the center of the secondary to return to the TEA laser cavity and/or receiver optics.

The coaxial receive beam of 300 mm OD and 200 mm ID is collected by 7, 5, and 6 and is focused by spherical mirror 1 on detector 16. Diagonal 2 and its support do not intercept any of the signal, since they are in the shadow of previous elements.

The low pressure flowing gas local oscillator laser uses a Littrow mirror 15, and a piezoelectrically controlled coupling mirror, 14, identical to the injection laser. And since they are identical, any systematic frequency shifts (such as that due to gas pressure and temperature effects) tend to cancel out in the receiver. Both lasers are dither stabilized, and the dither modulated signals are collected by beamsplitters 13 and 20 and are converted to AFC control signals by the dual pyroelectric detector, 18. The local oscillator signal is focused by the 50 cm focal length spherical mirror, 11, onto the detector. The resulting planar phase fronts on the detector are coplanar with those of the signal, although the LO spot size is intentionally considerably larger than the 100 × 100 micron detector.

Zinc selenide beam splitters 13, 20, 28, 10, and 9 are antireflective coated on one side to prevent interference effects, and they use the natural Fresnel reflection (about 30%) from the other side. Beamsplitter 9 is considerably larger than the laser beams going through it because it also serves as a manual boresight. An observer looking into 9 from the left sees the field of view of the receiver system. This is used as an alignment tool in the initial alignment procedure and provides a second convenient, mmagnified, boresight view for the operator. Either boresight, 8 or 9, can be used for a TV camera to provide a remote monitor of the laser interrogated field, although 9 is somewhat confusing because of the central obscuration. Beamsplitter 9 is also partially transparent at the visible wavelengths, which is very important for the periodic heterodyne alignment checks. In the heterodyne alignment procedure, an He/Ne laser is used to mutually align the TEA laser cavity, the injection laser, the LO laser, and the receiver beam for maximum heterodyne efficiency as well as for boresight alignment of the transmit and receive beams on the target. By using only multiwavelength optics, we greatly simplify this alignment procedure.

The TEA laser output is monitored by a very small pickoff mirror, 29, that deflects a 1 mm pie-shaped sector of the TEA laser output into the pyroelectric power monitor, 27. Beamsplitters 28 and 10 direct some of this signal, suitably attenuated by 17, into the detector where it heterodynes with the local oscillator (LO). This provides a consistent IF signal by which the piezoelectrically controlled mirror 33 can control the frequency of the TEA laser to match that of the injection laser and LO laser.

The optical bench layout consists of 40 precise optical components and their supports. Each support must provide for precise adjustment and stability and all the degrees of freedom necessary for optical heterodyning. Figure 14 is a machine-shop drawing of one of these, item 7, typical of the 40 separate items we have built. To realize this optical system, we made

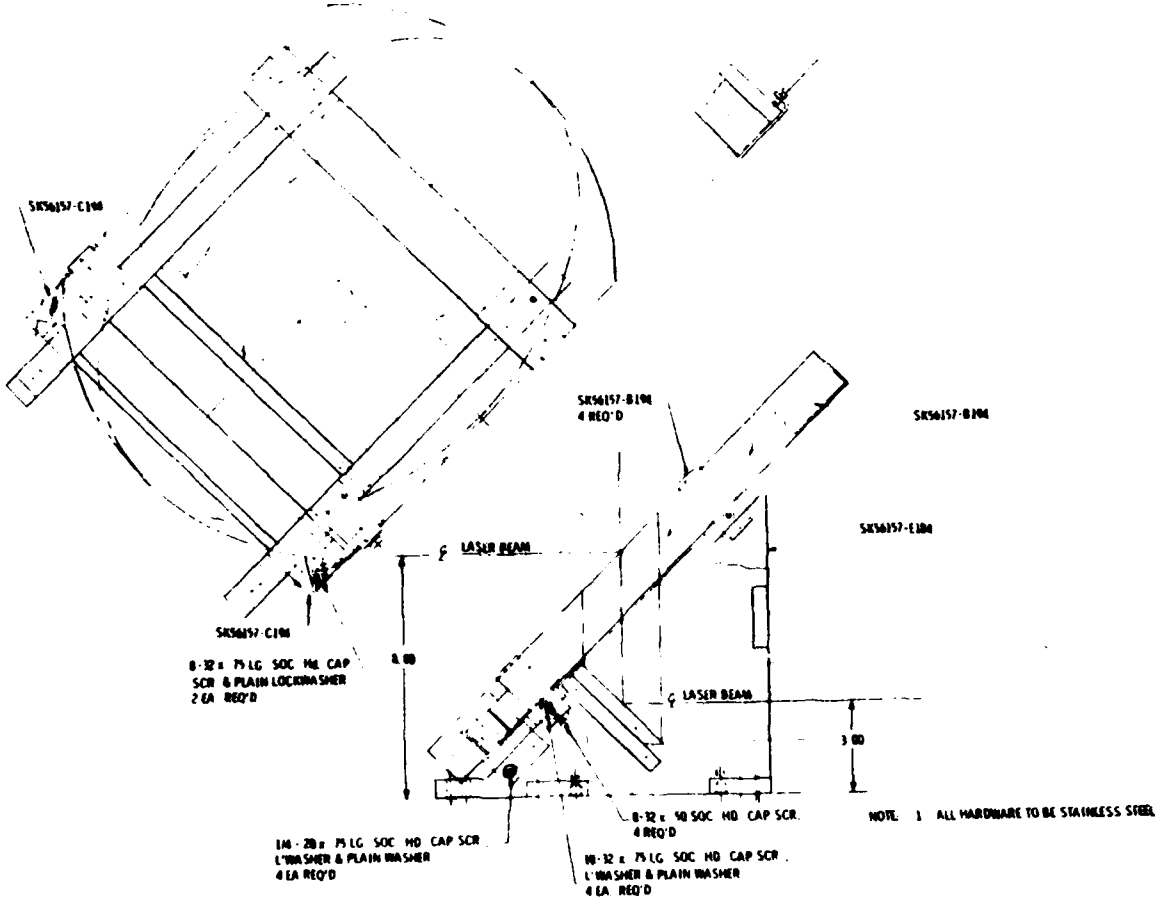

Figure 14. Twelve-inch Output-Beam Coupler

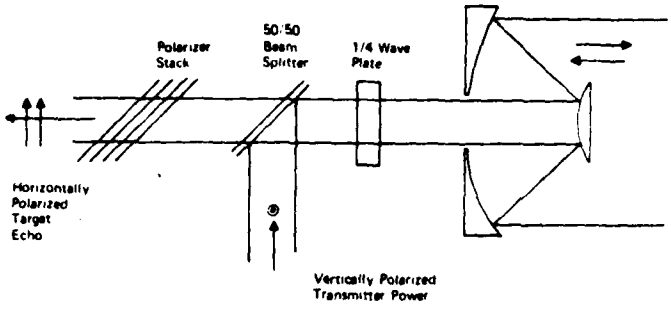

Figure 15. Polarization Isolation Duplexer

many tradeoffs and considered many design factors. Two of the most critical components in the design are the transmit-receive duplexer and the main beam expanding telescope. We touch on these design factors below.

4.4 DUPLEXER DESIGN

There is an elegant passive optical duplexer that uses polarization isolation between the transmitted and received beam (shown in Figure 15). The transmitted beam is converted to circular polarization by the quarterwave plate, bounced off the target, converted back to a linear polarization orthogonal to the transmitted pulse by the return passage through the quarterwave plate and then passed by the (Brewster stack) polarizer on its way to the detector. Spurious backscatter such as that scattered from dust on the 50/50 beam splitter is, in principle, stopped by the polarizer before it can get to the detector.

This scheme has several disadvantages, the first of which is a 6 dB energy loss from the beam splitter. Second, energy scattered from any object beyond the quarter wave plate such as the primary or secondary of the telescope, their supports, trees, leaves, buildings, or rain beyond the telescope is also converted such that it can arrive back at the detector. Putting a large quarter wave plate at the telescope output would require a very expensive waveplate and would still not stop the backscatter from buildings and trees. Further, our tests with these types of isolators, at visible wavelengths, showed that the isolation is at best only a few tens of dB.

The most effective type of duplexer is simply a fast-acting shutter. A rapidly rotating wheel with a small hole on the periphery synchronized to the transmitter pulse and at the focal point of a lens system preceding the

detector will eliminate all backscatter at any range. Because of the finite wheel speed and other mechanical limitations, the laser radar minimum range must be several microseconds. We have used these types of modulators in laser cavities at 10μ and found them reliable. An electro-optic pockel-cell type of modulator having very fast time can also be used to block off the detector at the time of transmission. This scheme is expensive, requiring high current, high voltage pulses, and a long crystal of gallium arsenide (GaAs) or CdTe. Its isolation by itself is only bout 40 dB, and it introduces 5 or 10 dB of losses in addition to those of the beam splitter.

Figure 16 shows the concentric mirror duplexer we have chosen. This may be augmented by the mechanical type should the need arise. The technique takes advantage of the fact that the TEA laser cavity output beam is already an annulus. Thus, there will be no specular back-reflection from the secondary center and no energy lost by the obscuration of the secondary. All the transmit power is expanded into a beam, in our case, about 160 mm. The receiver accepts collimated energy from a larger zone that is 200 to 300 mm in diameter and is spatially isolated from the transmitter beam by a buffer zone that is 160 to 200 mm in diameter. This receiver area collects almost 50% of the total signal that is theoretically available to the 12-inch diameter aperture, although there is of course S/N degradation due to mismatch of the transmit and receive beamwidths.

We think that careful control of the backscatter sources will provide a simple but safe system. Consider now one of the several calculations we made of possible backscatter levels. Assume the scanner is accidentally pointed at a building or other diffuse surface only a few tens of feet away from the transmit scanner, as in Figure 17. Note that the detector is at the focal point of the telescope, and although the illuminated annulus is in the near field beamwidth of the telescope, the fact that the detector is at the far field focus means that, in principle, no energy falls anywhere on the detector (if it is small enough). If d_1 were 100 feet and the focal length of the telescope, d_3, were 15 feet (F:15, 1 foot diameter objective), the distance d_2 would be $\frac{d_3\ d_1}{d_1+d_3}$ or 13 feet, and the maximum diameter of illumination, d_4, at the detector distance d_3 would be about

$$\frac{1}{13} \times 2 + \frac{.5 \times 13}{100}$$ or a quarter of a foot in diameter.

Although by ray theory alone no energy will fall on the detector, because of diffraction some energy would reach the detector. Since the diffraction field energy is a time consuming computation of Fresnel integrals, let us, for the moment, assume the worst case. Assume all of this return energy is uniformly scatered over this 3-inch diameter (44 cm^2). Since the diffuse surface is 100 feet away, the 1 foot diameter aperture would capture only a fraction $\frac{(.5)^2}{16(100)^2}$ or 1.5×10^{-6} of the reflected energy or about 10^{-6} for 30% reflectivity Lambertian backscatter. The total energy intercepted by the detector of 10^{-4} cross section and a 1 joule transmitted

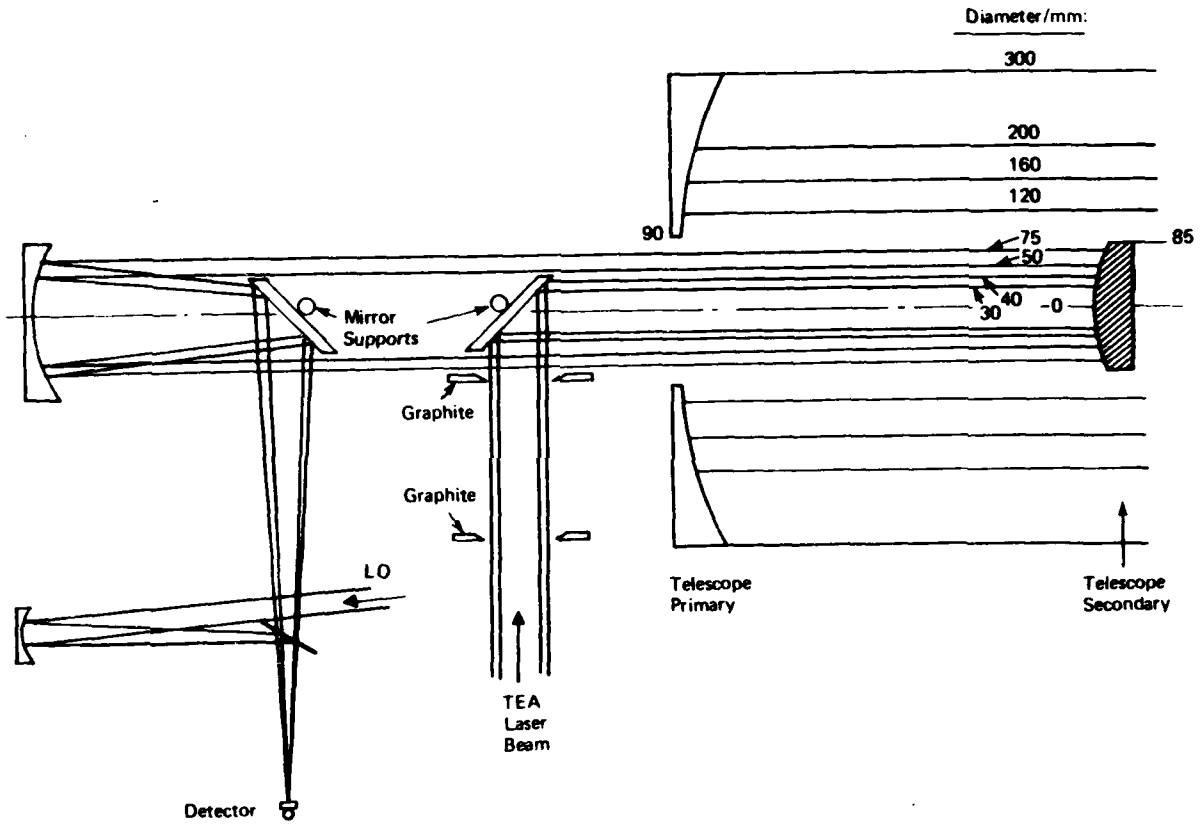

Figure 16. Concentric Mirror Duplexer

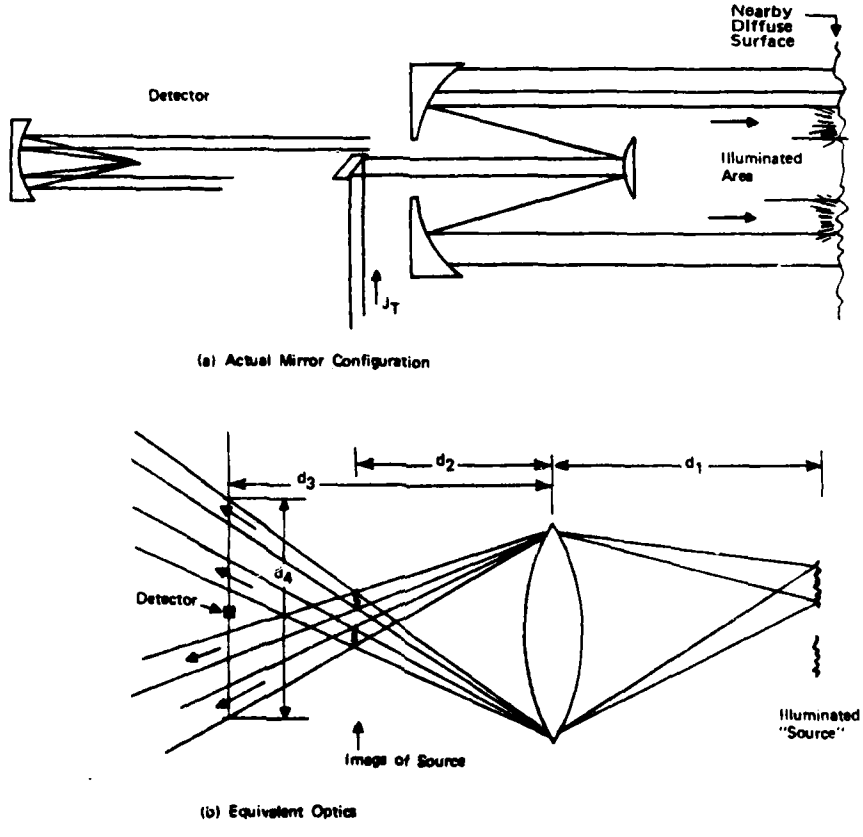

Figure 17. Detector Power in the Event of Illuminating a Nearby Diffuse Surface

pulse is thus only $\frac{1.5 \times 10^{-6}\ 10^{-4}}{44} = 3.5 \times 10^{-12}$.

This is well below the energy tolerance of 10^{-9} joules, (10 watts/cm^2, 1 μs).

In summary, it appears that, even for the unusually high power and large aperture of the AFGL radar, no active transmit-receive switch will be necessary, although several practical backup techniques are available.

4.5 SCANNER TELESCOPE

The function of the scanner telescope is to collimate the relatively high-power laser output coaxially with the receive beam such that both beamwidths are close to the 30 microradian diffraction limit of the 12-inch diameter objective. A reflective system has advantages over refractive optics of power handling and cost. The Cassegrain has advantages of physical size and cost over the other reflective telescope configurations. Since our TEA laser cavity output is already collimated (confocal) and annular (unstable), it makes a natural obscuration. The design questions are now reduced to a selection of focal length and figure.

A parabolic primary and parabolic secondary, on-axis, provide perfect (diffraction-limited) beams. Because of the high laser power, our convex secondary should be made of copper. But to grind a convex parabola, particularly in metal, is expensive since it requires a matching parabola for testing. Thus, our secondary must be spherical. Saddled with this requirement for a spherical secondary, we need an aspheric primary to recover the beamwidth. The optimum Cassegrain configuration using a spherical secondary is known as Dall-Kirkham, in which a spherical primary is modified to an ellipse. Dall-Kirkham results in a major improvement in beamwidth over sphere-sphere and the touch-up grinding required for it is less than for a parabola. We need some numbers by which to estimate the optimum configuration.

The equation of a parabola whose vertex is at (0.0) and whose collimated beam is horizontal is

$$x_p = \frac{y^2}{2r_o} ,$$

where r_o is the nominal radius of curvature at the x axis.

The equations of the sphere (which of course represents the shape of the mirror as it comes initially from the grinding and polishig machine) is

$$x_s + \frac{y^2}{2r_o} + \frac{y^4}{8\ r_o^3} + \ldots .$$

The difference, $\frac{y^4}{8\ r_o^3}$, is an indication of the spherical aberration. If

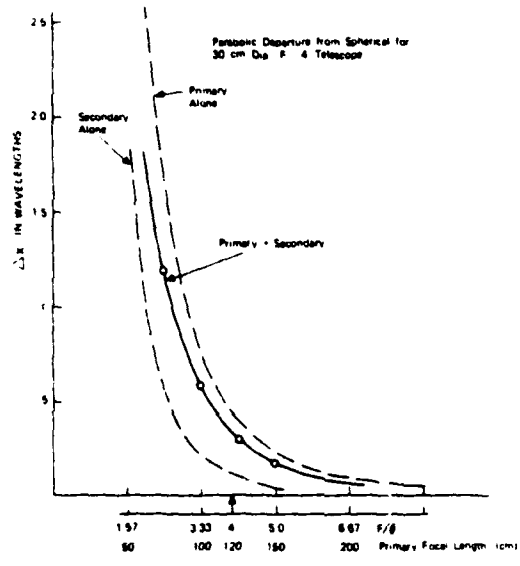

Figure 18. Spherical Telescope Figure Error

this difference is less than a quarter of a wavelength at the rim, the mirror will in general give a diffraction-limited focus. And if the difference in the error between the secondary and primary is less than a quarter of a wavelength, the pair will give an output beam collimated to within the diffraction limit, (λ/D).

Figure 18 shows the difference between the (partially compensated) primary and secondary for a telescope having a 12-inch diameter primary and a magnification of 4. It can be seen that an F:4 system is nearly diffraction limited (Δx = .3) and is sufficiently short (120 cm focal length and 90 cm between primary and secondary) that it can conveniently sit on our optical bench. To get the maximum heterodyne S/N, however, we should specify a Dall-Kirkham aspheric for the primary. Figure 18 shows that the glass to be removed for a parabola is about 0.1 wavelength at the rim. The Dall-Kirkham ellipse will require aspheric polishing of about half this .05 wavelength at 10μ, or one wavelength in the visible. The result will be a diffraction-limited system that suits both our bench and our pocketbook.

The F/4, magnification 4 telescope not only fits our bench; the collimated input laser beam matches one laser beam diameter of 40 mm and allows a safe 5 millimeters clearance between it and the receive beam (see Figure 15). Our TEA laser cavity beam with a 40 mm OD is necessary to extract efficiently the power available in the active laser gas volume. Although the beamwidth of this telescope is diffraction-limited when the axes of the two mirrors, the laser cavity, and the heterodyne receiver are perfectly aligned, and when the telescope is focused for infinity and observing a target at infinity, there is some question about what the beamwidths will be for conditions other than these. That is not to say that

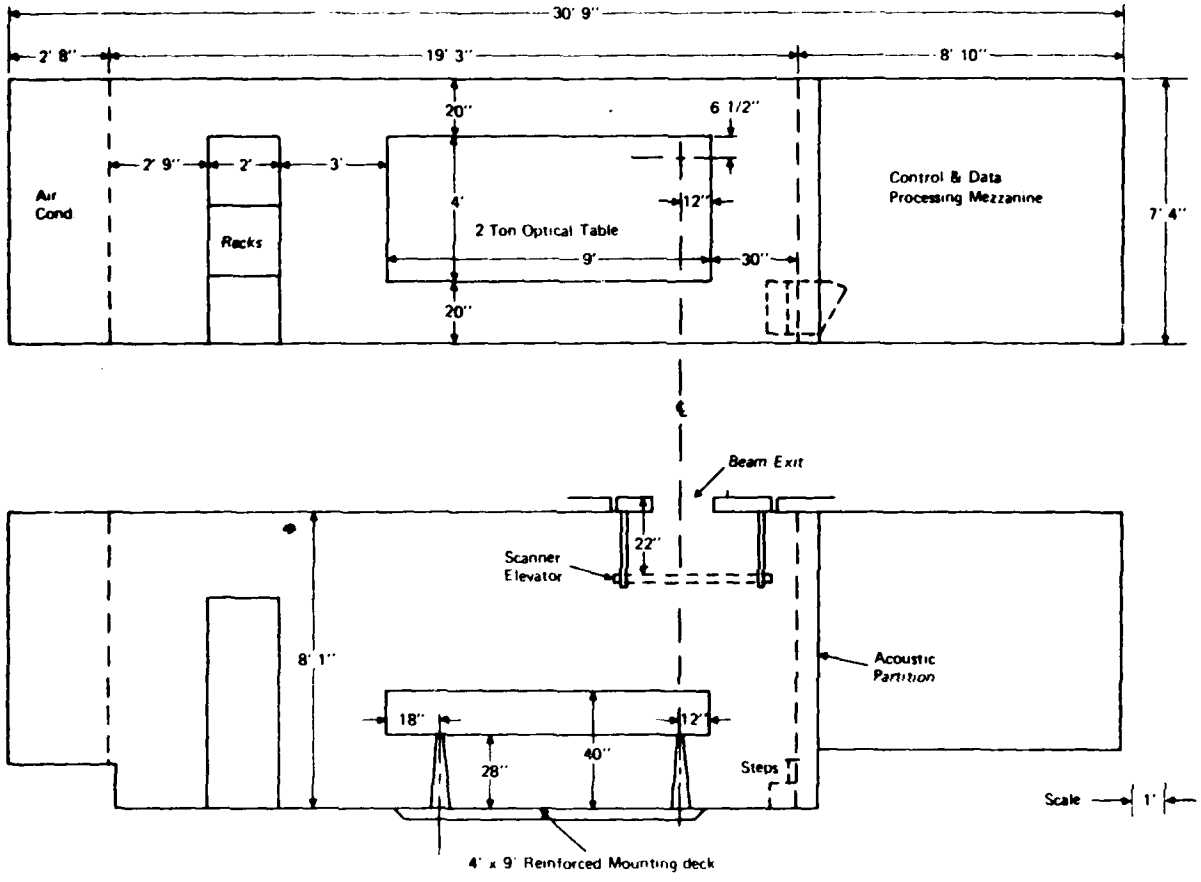

Figure 19. Inside Dimension Requirements

any other simple telescope configuration can provide higher tolerance to off-axis or unfocused conditions, but we need the effect of these conditions to know what alignment precision is needed in the system setup. To this end, we have started to construct a computer program for the off-axis and "focusing" aberrations of the Dall-Kirkham. This should be complete in time to assist in the optics assembly and testing.

4.6 TRAILER

In April, General Electric sent AFGL a series of sketches and notes showing the planned laser system configuration and the recommendations for the design and construction of the GFE trailer. We briefly summarize those ideas here as an indication of our plans for the final trailer layout.

4.6.1 Inside Dimension Requirements

The overall space requirements (shown in Figure 19) are dominated by the heavy optical bench, to which one needs access on all 4 sides. The bench is a 12-inch thick honeycomb table that holds the optics and the 700-pound TEA laser (Figure 19). We need all the room underneath (28-inch) available for vacuum pumps and power supplies. We suggest a flush bolt-plate to which we can fasten all components. Because the table does not have separate vibration isolators, it is essential that the air-ride suspension system be soft. The laser beam leaves the table vertically and goes to the roof-mounted scanner. This beam must stay centered into the scanner to within a 1/4" on the center line shown.

Because the TEA laser makes an annoying pinging sound, we suggest an acoustic (wall) barrier between the laser room and the control room. We plan adequate protection from lethal voltages and laser power, but because there are many voltage and laser radiation hazard areas above and below the laser table, we suggest enclosing the whole optical bench with sliding plexiglass doors from floor to ceiling.

At times, it is necessary for operators to adjust the optical components with the power on. In our experience, this is not dangerous, if it is done by an operator who understands the system. But to individually enclose every hazard above and below the bench would in the end be more dangerous because of its inconvenience.

The scanner elevator is intended to lower the scanner for travel or bad weather. The vertical columns must be stiff enough to hold the lowered scanner in travel. When raised, the scanner must return to within ± 1/4-inch of its original position. A 4-cable manually driven drum winch could be used to hold the elevator horizontal when the scanner is being raised.

4.6.2 Air Conditioner Heat Load

We estimate the heat radiated by our equipment, into the room, will amount to 7 kW.

4.6.3 Tanks of Premixed Gas

Four or five tanks of premixed high-pressure but non-flammable gases will be used to operate the CO_2 lasers. A duct under the floor is needed to carry the gas from the tanks to the lasers. Location of the duct (and water pipes) should conform to plans since the spacings are close.

4.6.4 Scanner Clearances

Figure 20 shows a cross-section of the roof top, scanner and the overall clearances it will require. Figure 21 shows the dimensions of the elevator required for the scanner's clearance. Note that the entire scanner rotates on the azimuth bearing to provide azimuth scan, but elevation scan requires only the movement of the elevation mirror. In both cases, the beam rotates on a one-to-one basis with the mirror, not two to one, as in the usual mirror scanner.

4.6.5 Cooling Water Requirements

The cooling water can be either constantly replenished from a well or municipal system or cooled with a refrigerator and recycled. Total flow rate is 4 gpm at about 50°F.

4.6.6 Power and Control Ducts

We need 15 kW, 4-wire, 3ϕ, 208/120V at the racks and about 2 kW, 120V at the table. One of the racks holds a power supply that requires 1 kW, 120V single phase. It is desirable that the power for this unit be regulated to 0.5%.

4.6.7 Power and Control

Figure 22 shows the power and control panels located next to the air conditioning system (Figure 19). This consists of three standard racks positioned so that there will be easy access to both front and back for maintenance. By locating the panels next to the air conditioning apparatus, a single access "hallway" can be used to obtain access to both kinds of equipment.

The power and control system uses three standard 19-inch racks, two of which are devoted to the power supplies and their controls. The third rack is used for the control and signal electronics. This includes the three AFC systems, the scanner azimuth and elevation position controllers and angle displays, and the pulse trigger system.

The major power requirement is 5 kW for the TEA laser sustainer. This provides a nominal 20 KV, DC to the sustainer power capacitor located under the optics bench. The next power requirement is 2.5 kW for the electron gun modulator. The modulator control is on the center rack. The 25 KV DC power supply itself is in an oil filled container under the table. The thyratron/PFN pulser is in another oil filled box under the table. The

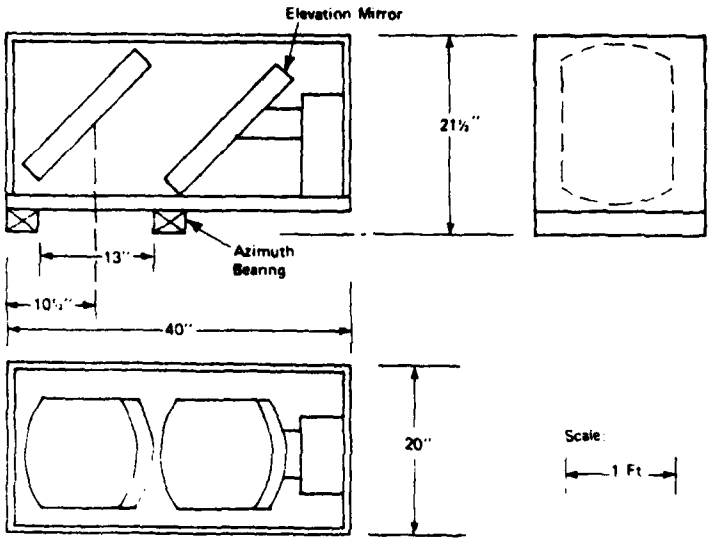

Figure 20. Scanner Cross Section

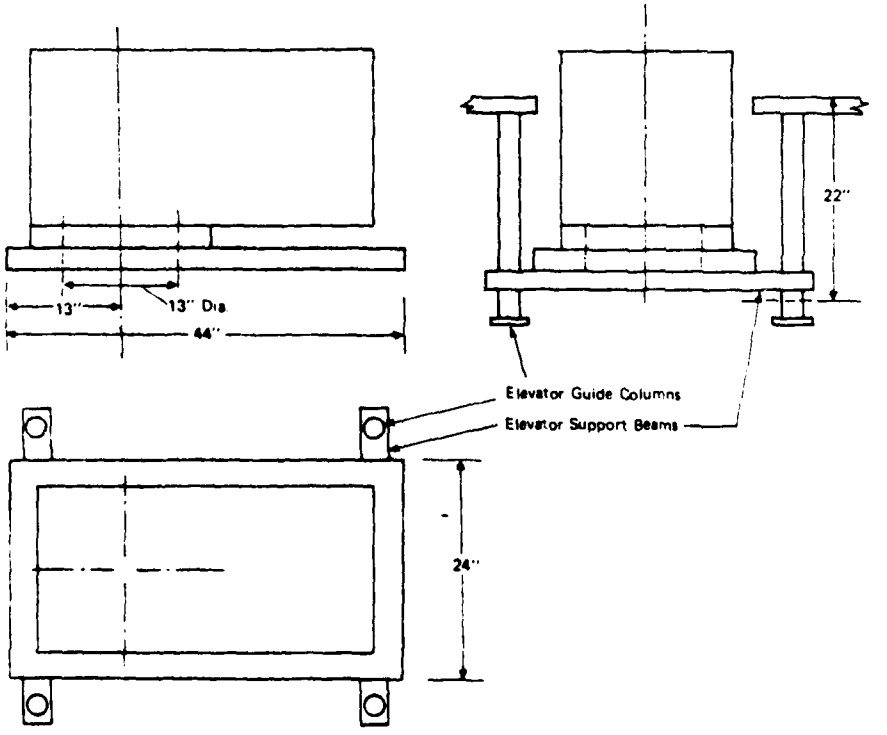

Figure 21. Scanner Elevator

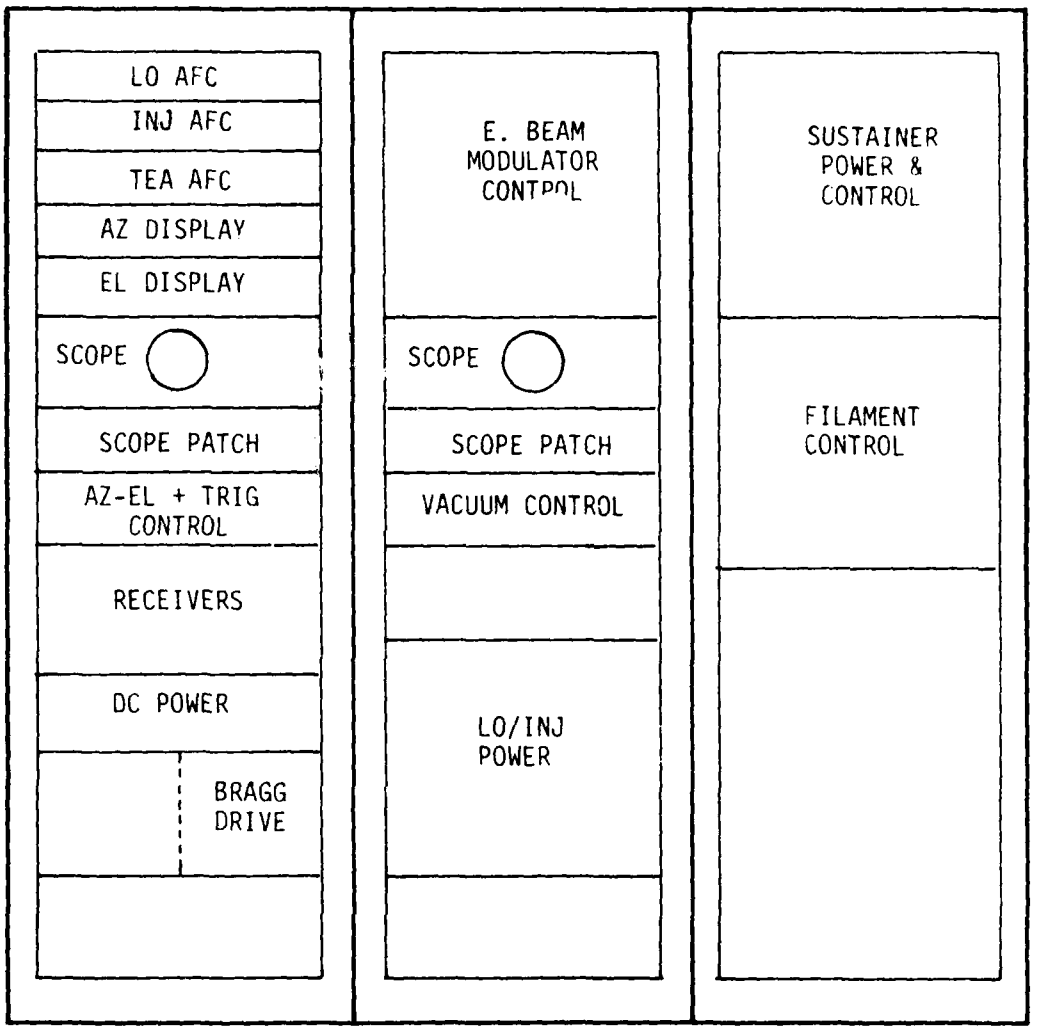

Figure 22. Laser Power and Control Panels

power supply for the injection and LO lasers (25 KV, 40 ma) is in the center rack and should have regulated primary power (120V) to enhance AFC frequency stability.

The three racks in Figure 22 are the center for controlling and monitoring, and they house almost all of the electronics. The functions associated with each panel are as follows.

The left rack houses the three AFC units which are modified Lansing, 80.215 lock-in stabilizers. Below these are the two Computer Conversion Corp. units that convert the customer azimuth and elevation commands to analog format and display the resulting beam pointing angles.

We provide Tektronix 2213 oscilloscopes in the left and center racks to allow the operator to monitor the system operation in considerable detail. In practice we have found that one scope should show the laser pulse shapes such as sustainer current and output power and the other should monitor critical "support" functions such as AFC error signals. Under each oscilloscope is a patch panel allowing each scope to be quickly switched to any of about 10 signals. These scopes are only good to 60 or 80 MHz and are not as bright at the 50 Hz basic pulse repetition rate as we would like. They will, however, provide a convenient center for parameter checks and operator confidence monitoring. The patch taps are BNC and available to more sophisticated test instruments that might be needed on a temporary basis. The patch points are as follows.

Left Rack:

AFC IF Output
AFC Discriminator Output
AFC Sample and Hold Output
Log IF Video
Log IF IF
TEA AFC Gate Pulse
Bragg Gate Pulse
TEA Pyro Electric Detector

Right Rack:

E-Beam Modulator Current
E-Beam Modulator Voltage
Sustainer Current
LO AFC Monitor
Inj. AFC Monitor
Bragg Gate Pulse
AFC Sample and Hold Output
TEA AFC Gate Pulse

Below this on the left rack is the AZ-EL control chassis which allows the beam to be pointed manually and contains the servo op amp. This unit also contains the 5-channel trigger pulse generator, Figure 23, and their control.

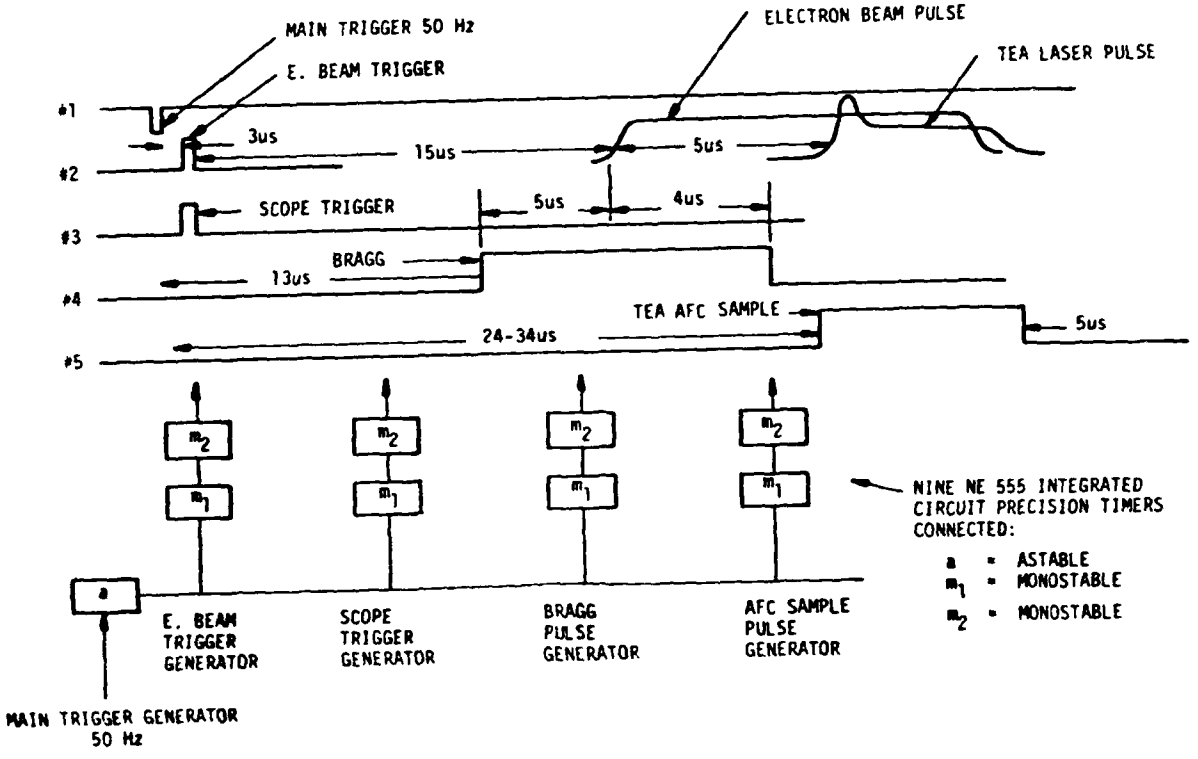

Figure 23. Pulse Trigger Electronics

The receiver, located below this, contains two IF amplifiers, two discriminators and the mixer and various couplers. It also contains the 110 MHz LO oscillator, the AFC sample and hold gate and the 40 MHz Bragg oscillator and switch. The latter feed the 25-watt Bragg driver locate at the bottom of the rack. The Bragg driver is interlocked to the temperature sensor in the Bragg cell itself.

Two low voltage DC power supplies service the various electronic chassis with ±15 volts 3 amps for the receivers and pulse generators and ±24 volts 6 amps for the AZ/EL op amps and various relays.

At the top of the center rack is the control panel for the 120 KV electron beam modulator. This unit is enabled by several internal interlocks such as thyratron heater and a control that prevents PFN pulse length change when power is on. An external interlock "is electron gun filament on?" will prevent excessive transients.

The electron gun filament control (variac) and current monitor is in a vacant area of the sustainer power supply panel, the right rack. This supply generally controls the laser power output by setting the electron beam current. The supply is interlocked externally to several conditions, "Is gun cooling water flow rate adequate", "Is gun vacuum below 2×10^{-2} torr?"

In the center of the center rack is the vacuum control panel which contains a thermocouple vacuum gate and controller and an ion vacuum gage. The latter monitors loss of vacuum due to filament outgassing and foil leaks, and the former serves as the interlock signal to turn off the roughing pump, the diffusion pump and filament power if the foil ruptures during operation or when the system is unattended. The diffusion pump is disabled if its cooling water drops below the required flow rate.

The lowest panel on the center rack is the high voltage for the injection and LO lasers. The only external interlock for this is cooling waterflow.

The right rack is the sustainer power which is interlocked to cooling water in the heat exchanger and power to the TEA laser gas circulation fans.

4.7 SCANNER POSITIONER

Figure 24 shows the partially completed assembly detail of the azimuth and elevation bearing support and drive system. Both axes are driven by geared-down DC motors, and both motors are coupled to the driven axis by non-slip belts (polypropylene and steel cable formed into a chain). To isolate the strains owing to driving torque from the angle readout, the synchro shaft encoders are coupled to the axes with a separate smaller "chain". In the case of the azimuth encoder, the chain ratio is 10:1, and a suitable 1:10 gear inside the azimuth synchro provides the net 1:1 readout. This gearing is required because of the large (12-1/2 inch) diameter azimuth throat required to accommodate the 12-inch diameter telescope beam. The chain drive and power system has been designed to provide the required

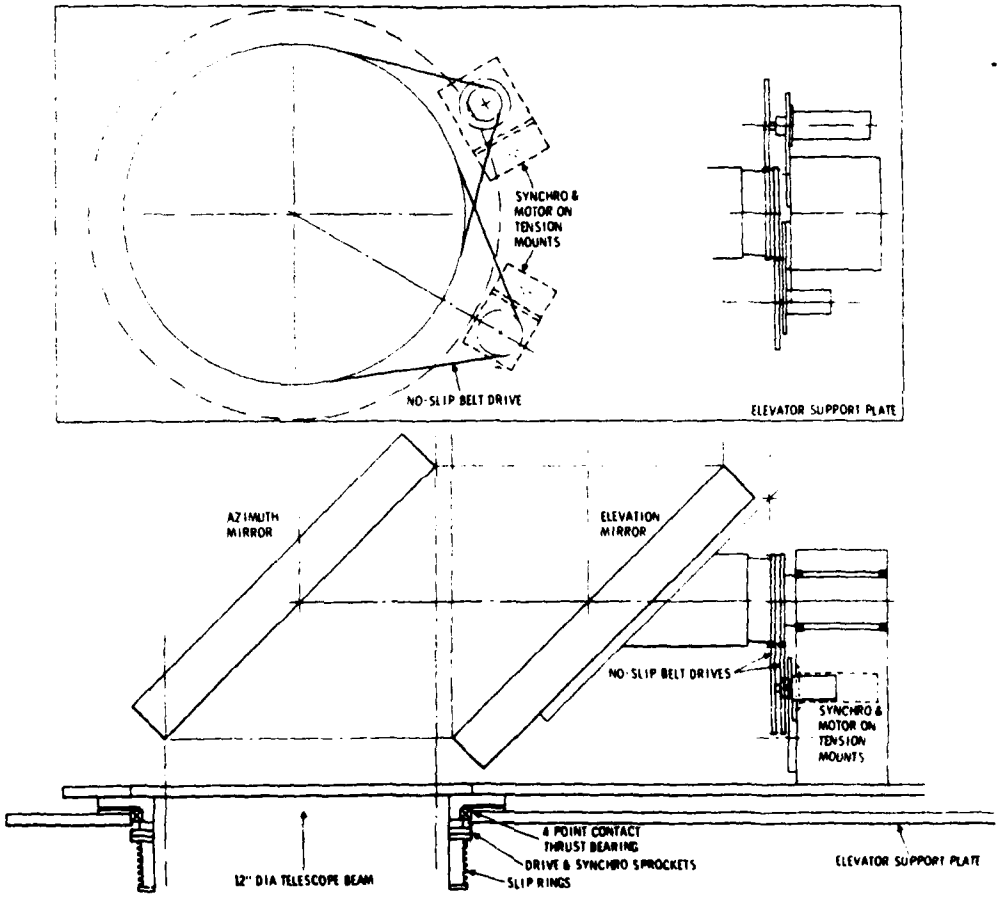

Figure 24. Scanner Bearing Detail

.25° precision and .1° stability in the face of a 10 mph wind. Since the maximum rotation rate is only 2 rpm, the drive motors need only be about 1/30 hp.

In the position control system, the command position angle from the computer is compared with the actual azimuth (or elevation) position indicated by the synchro shaft angle encoder and an error signal is generated. The error signal drives the motor in a typical servo loop to put the mirror into the command position. In alternate modes, the motor can be set manually to a desired position or constant azimuth and elevation scan rates. A synchro rather than an optical or mechanical digital angle encoder was selected to avoid a large number of slip rings on the huge 13-inch diameter azimuth bearing.

The decision to use a servo motor control system rather than an open loop stepping motor was based on several factors. The main factor was that a stepping motor occasionally misses a step, particularly with high inertia loads such as these or when the power is turned off. Other factors were the need for ramping the stepping rate and converting the computer's binary parallel output to the serial step format required for stepping. Lastly, separation of the angle encoder and motor drive allows better accuracy in the angle position in the presence of buffeting winds and accelerations. Angle errors due to motor drive structure are not controlled in a system in which the motor is its own angle encoder.

The technique by which we match the customer's digital position command to an analog servo is shown in Figure 25. The azimuth or elevation position as measured by the synchro is converted to 14-bit parallel binary by the resolver to digital converter, R/D. The instantaneous digital position is compared with the digital command (from the computer or manual input) and an error signal generated, by the subtractor. This 14-bit parallel error signal is converted to a ±10 volt analog signal by the D/A. The analog error signal is amplified by a power op amp to the several ampere current level necessary to drive the AZ/EL motors. The loop is closed mechanically and the error driven to zero.

The digital position from the R/D is also presented as two outputs. This 14-bit binary parallel angle position goes back to the customer signal processor and it goes to a display unit which presents the instantaneous angle in degrees decimal to the local operator. This system was prepared from "standard" components by the Computer Conversion Corporation and represents a low cost method of getting high accuracy and assurance that the various digital modules will match the time, voltage and encoding format.

The power op amps, AM8530, are supplied with ±24 volts. The motors, Globe Type BD, 100A104-100 and Type LL, 3A1003-1 for azimuth and elevation respectively, are high ratio gear motors only an inch or so in diameter.

The azimuth servo (Figure 25) is the same as the elevation system except for the multiturn requirement imposed by the large azimuth sprocket. In both cases, a large gear ratio (approximately 5000:1) between the motor

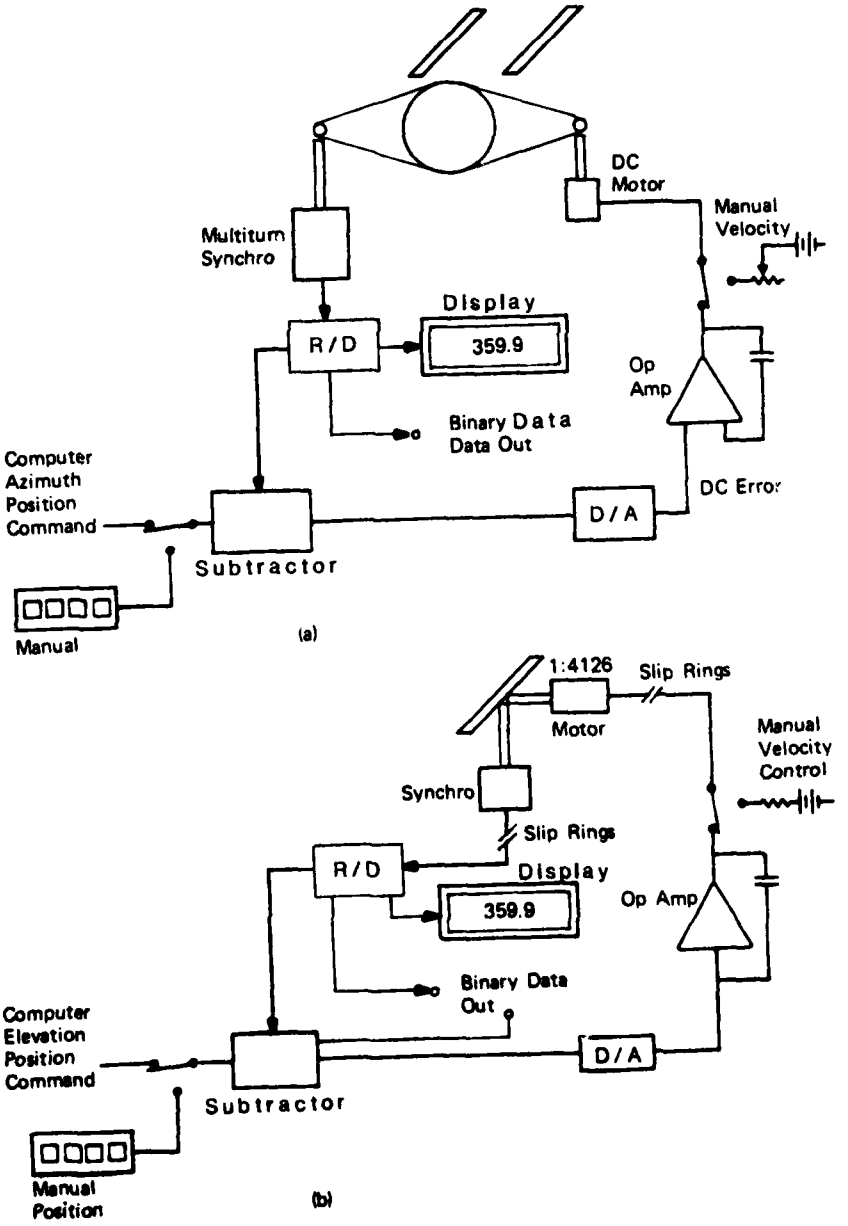

Figure 25. Digital Position Command Servo
a) azimuth b) elevation

and the driven mirror reduces the equivalent angular momentum of the load to be comparable to that of the motor. Thus, the servo's crossover frequency should be comparable to that of the motor's frequency response of several radians per second.

This is a Type I servo system in which high stability and transient response can be achieved by a simple lead or, as shown in Figure 25, lag network in the op amp stage. Because the lowest bit of the binary output of the angle encoder can be easily converted into a rate signal, the system also has the potential for a simple rate stabilization feedback network. By avoiding the backlash of large ring gears or hard chain we believe the completed system will not have a hunting problem. But we plan servo measurements and refinement once the system is built and set up.

4.8 ELECTRONICS

The "electronics" system as defined in the lower portion of Figure 1 contains two subsystems: the pulse timing system and the IF receivers. The electronics of the three AFC systems, the E-beam modulator and the scanner pointing system, were described previously.

The "receiver" of Figure 1 is actually two receivers. One of low sensitivity to measure the frequency of the TEA laser and provide an error signal to the TEA AFC and one of high sensitivity to measure the amplitude and doppler of aerosol and other target returns. The AFC receiver uses a linear IF and uses a low IF gain to avoid the FM noise generated between pulses that would tend to cause errors in the AFC. The high gain receiver uses a logarithmic IF to accommodate the enormous dynamic range of expected signals. The preamplifier between the detector and the two IF amplifiers has a 10-100 MHz bandwidth. Thus the doppler range of frequencies from 30 to 50 MHz is accommodated without distortion. By heterodyning these signals to the range of 60 to 80 MHz the signals are amplified further in the high gain receiver without distortion. Figure 26 shows more details of the two receivers.

The first mixer of the receiver is really the HgCdTe cryogenic optical detector. Made by New England Research, this unit has two unusual features. It has a 6-hour dewar and it has two detectors for the price of one (side by side but separated by one millimeter). S-10 (designated S-10 and S-8,) is 0.25 mm dia. and S-8 is 0.2 mm.

The detector is biased at a level sufficient to keep the frequency response well above the 30-50 MHz signal range. The signal is fed to the preamplifier with leads having a minimum of stray capacitance since the detector impedance is quite high (300-1000Ω). By using a preamplifier of as low a noise figure as possible the LO laser power is minimized and with it the risk of excessive heating of the detector under conditions of excessive transmitter backscatter or loss of cryogenic detector cooling.

The function of the LO laser power is to raise the signal level above the thermal noise until the system is dominated by the photon noise. The usual relationship for the required detector LO current is

$$I_o > \frac{2KT_o}{q}\left(F + \frac{T_d - T_o}{T_o}\right)G_p$$

where

K = Boltzmann Constant (1.3×10^{-23})

T_o = Standard Temperature (293°)

q = Electron Charge (1.6×10^{-19})

F = Preamplifier Noise Figure, (1.58 for a typical 2 dB noise figure)

G_p = Detector Dynamic Admittance (typically 10^{-3} mho)

T_d = Detector Temperature (77°K)

This works out to about 40 microamperes which requires only 15 microwatts of LO laser power at 33% quantum efficiency.

Unfortunately the above equation assumes an impedance match between the preamplifier and the detector. If a standard low noise preamplifier is used, it will have a 50 ohm input impedance. If a high impedance FET amplifier is used, it will have a far worse noise figure in the frequency range of interest. And to obtain a wideband transformer to go from 1000 down to 50 ohms is quite difficult. Related to this is also the task of biasing the detector at the level of minimum noise, approximately zero volts across the detector, taking into account the LO induced current. The best compromise seems to be simply to use about 1 milliwatt LO power, RC coupling to the detector and a commercial low noise wideband amplifier. We note that the coupling capacitor capacitance must be as low as possible to avoid damaging transients when connecting up the detector and low bias power.

The preamp selected is an Anzac AM113 of 2 dB noise figure. The equivalent noise is

$$T = \Delta T + T_o = (NF-1)\ 300 + 72 = 254°.$$

The resulting noise current in the preamp is

$$I_{NA} = \sqrt{\frac{4KTB}{R}} = \sqrt{\frac{4 \times 1.3 \times 10^{-23} \times 254 \times 2 \times 10^{7}}{50}}$$

$$= 73 \text{ na} .$$

The photon noise due to the LO current is

$$I_{NN} = \sqrt{2QBI_o}$$

that is

$$72 \times 10^{-9} = \sqrt{2 \times 1.6 \times 10^{-19} \times 2 \times 10^{-7} \times I_o}$$

which solved for I_o gives an LO induced detector current of 0.825 ma. This in turn requires a LO laser power on the detector of about 340 μw at a quantum efficiency of .33, or about a milliwatt allowing for spillover.

Thus we can assume that the minimum detectable signal into the preamplifier is about 100 na or -93 dBm as listed in Figure 26. After traversing the AM-113 preamplifier, and 3 dB coupler the signal is -65.4 dBm. The conversion loss, L_c, of the mixer, assuming a +7 dB signal from the 110 MHz "second" LO, is 6 dB which provides an overall mixer noise figure of

$$F_o = L_c (T_r + F_{IF}-1)$$

$$= 4 (1.5 \times 4-1) = 18 (12 \text{ dB})$$

This is equivalent to a mixer input noise level of -82 dBm which is well below the expected minimum signal.

The 60-80 MHz log IF (an RHG type LST) has a dynamics range of -75 to +5 dBm. Thus a small, 3.6 dB, input attenuation will maximize the target handling capability.

The video output from this IF to the customer signal processor will range, (linear in dB), from 0.25 to 2.5 volts over this extent. The IF output however will be essentially hard limited at 0 dBm for all signals above -60 dBm. This makes a nice match to the subsequent frequency discriminator, an RHG type DT. The discriminator will provide 0.1 volts/MHz output over the ±10 MHz doppler range.

The AFC channel is similar except that the IF (RHG type ICFV) is linear to avoid FM noise. We have assumed that the AFC mirror pickoff on the TEA laser output (item 29, Figure 8) and the attenuators (item 17, Figure 8) will be set at a level to produce a detector output of -53 dBm which places the signal into the linear IF at -25.4 dBm and a signal of -8 dBm into the AFC discriminator when the IF gain is manually set at 20 dB. This level is midway in the AFC discriminator dynamic range of -20 to 0 dBm, which should allow a wide latitude of TEA laser output adjustment without affecting the AFC stability.

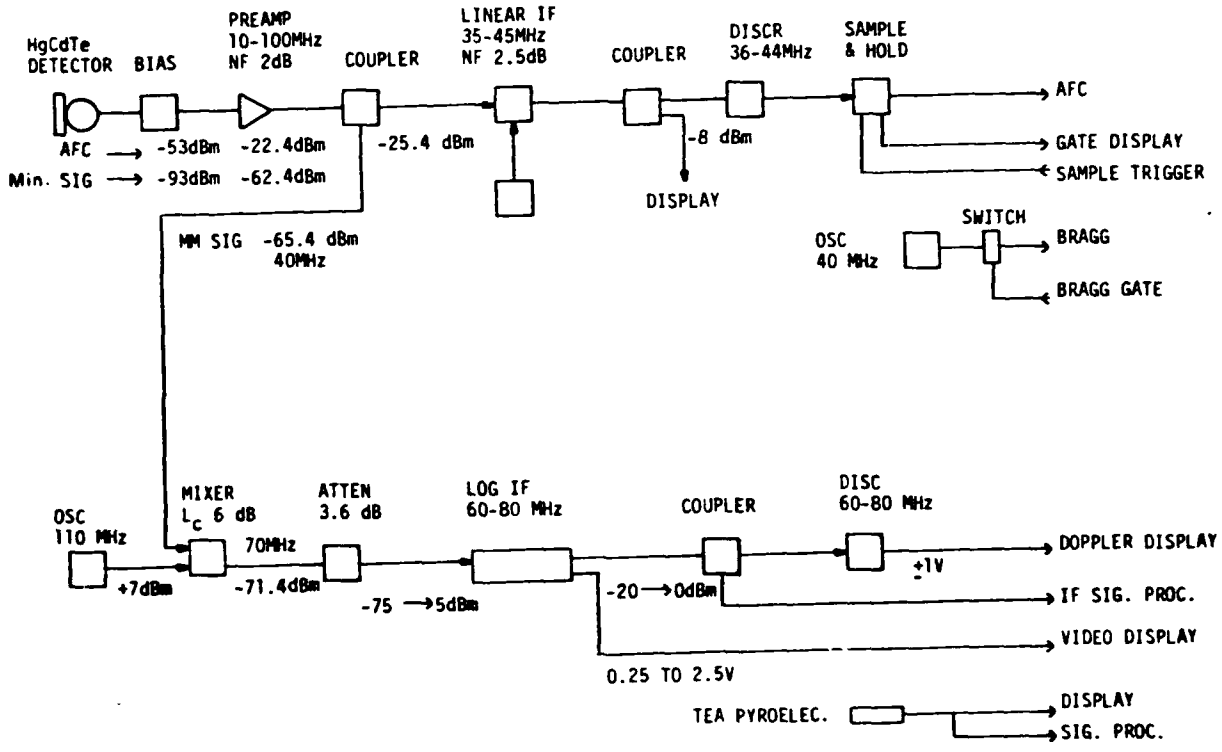

Figure 26. Receiver Electronics

For safe operation of the cryogenic detector the total incident optical power level should preferably not exceed about 10 w/cm^2 (or 1 milliwatts). This will give a signal of -10 dBm which is a potential dynamic range of 83 dB. This matches the range of the log IF but somewht exceeds the capability of the AM 113 whose maximum output is only +14 dBm.

The electronic LO is an EMF 5006 which is a mechanically tuned oscillator having a tuning range of ±16.5 MHz and a stability of about .01 MHz per degree C. This will probably be adequate for the customer signal processor since the pulse to pulse frequency jitter, which is much larger, will probably be accommodated by the signal processor which normalizes on the frequency of the AFC pickoff (zero doppler) IF.

Also shown in Figure 26 is the 40 MHz Bragg drive oscillator, (also EMF 5006) and the switch by which the Bragg driver is gated on for the 5 or 10 μs injection period. This is simply another mixer operated as a quad diode switch.

A pyroelectric detector also shown in Figure 26 (Item 27, Figure 8), will provide a measure of the TEA laser output.

The master pulse generator provides 0 to 50 pulses per second (about 1 μs long) to trigger the E-beam modulator. When the TEA laser gain rises to the point at which it is susceptible to injection of a "seed" pulse from the injection laser, the Bragg modulator is "opened." The Bragg cell is closed before the TEA laser output gets sufficiently large to affect the injection laser's frequency. At the same time, the output of the TEA AFC heterodyne receiver IF discriminator is gated into a boxcar to provide an error signal for the piezoelectric translator in the TEA laser cavity. The timing of this gate is important to block off any RFI signals early in the TEA laser operation period, to block off any doppler-shifted target returns after the main TEA laser pulse, and to block off FM discriminator noise when no signal is present. The boxcar is essential to generate an error signal sufficiently long in time to allow the AFC driver to respond. As shown in Figure 26 the gate and box car will be provided by a sample and hold circuit. The sample and hold device will be either an SHM-6 or SHM-iC-1. The advantage of the latter is that for a 2 μs acquisition time it has a droop of only 0.5 volts per second compared to a 5 V/sec droop in the former. The advantage of the former is that it can acquire this sample in about 1/2 the time. Neither parameter is critical however and the design will be chosen shortly. Present plans are to set the gate period permanently at 5 μs (irrespective of transmitted pulse length) but have a panel control by which the gate is set to bracket the transmitted pulse.

The pulse trigger electronics, Figure 23, is extremely simple consisting of 9 NE555 integrated circuit precision timers (voltage comparator plus flip-flop) made by TI. One is used in an astable mode as an oscillator generating the 0 to 100 pulses repetition rate. Four others (m_1) are used to generate a delay of from 3 to 34 μs and four more (m_2) are used to generate the gate or trigger pulses themselves. The 10-volt 50-ohm output of these devices provides a signal far above any RFI level.

The advantage of the EBI TEA laser is that its output frequency during the pulse is extremely constant. However, the frequency difference between the TEA laser and the LO laser jumps around from pulse to pulse by as much as 1 MHz.

Because of the AFC pickoff, the range zero Doppler signal can be used to correct for this frequency jitter. Thus, when the range zero Doppler is compared to the 40 MHz electronic reference oscillator, the frequency jitter can be accurately measured and used to correct the target data. If, in the future, this pulse-to-pulse jitter is inconveniently large, it can be reduced by modifying the TEA laser system. With this technique, we would use the injection signal to measure and set the TEA laser cavity before the TEA laser pulse.

4.9 HETERODYNE LASER RADAR TECHNIQUES

Alignment test and operation of this laser radar will require techniques and adjustments to the system characteristics of no more complexity than any coherent optical system. Yet, there are specialized techniques that are not common knowledge or are peculiar to ten microns that warrant some discussion. One of the most common technique problems, for example, is tracing the path and shape of a beam that is invisible to the eye, especially if the power level is too low to be made visible by UV fluorescence inhibiting devices, thermofax paper or other thermal techniques.

TEA Cavity Alignment

The TEA laser cavity must be aligned in several degrees of freedom most of which can be set, in our system, with an He/Ne laser. A nearly collimated He/Ne beam of about 3 milliwatts injected with a separate mirror at a point between 30 and 31 (Figure 8) will traverse the cavity repeatedly clearly showing its path by the light scattered from the mirror surfaces. Adjustment of the beam to close upon itself will be sufficient alignment to allow the TEA laser to oscillate when it is energized.

Now by following the He/Ne beam as it is removed from the cavity by the scraper mirror, 32, the beam can be aligned to center on the diagonal, 33 and the secondary 6.

To align the TEA laser-telescope combination on the target, one can put a mirror between TEA laser mirror 31 and 36 and look along the cavity towards a nearby target with the boresight telescope.

The receiver system is aligned in two steps. First the LO laser beam is placed on the detector, colinear with the expected receive beam, then the receive beam is aligned on the nearby target, colinear with the LO beam by looking into the beam splitter, 9.

Once this initial alignment process is completed with the visible beam, the alignment is improved by heterodyning at ten microns in two steps; first, using the LO and injection laser only and then using the additional power of the TEA laser.

The injection laser is collimated with the TEA laser cavity using a pyroelectric detector in the cavity and looking back toward the injection hole in mirror 31. Then with a corner reflector as target--at say 1000 foot range the target is observed on the ten micron heterodyne receiver. Realigning the main telescope on the target for a peak will align the transmitter system. Realigning mirror 2 for a peak will align the receiver system.

The last step is to repeat the alignment of transmitter and receiver, as above, using the TEA laser power and a spherical rather than retro mirror target. To avoid damaging the cryogenic detector an unknown signal should be measured with liberal use of ten micron attenuators. Three mil Kapton has an attenuation of about eight.

The Bragg modulator pulses the output of the injection laser and shifts its frequency 40 MHz. The Bragg angle deflection, between the undeflected, straight-through, beam and the acoustically deflected beam is 77 milliradians. At 12 watts of power applied to the modulator about half the incident laser power appears in each beam. Since the laser energy is focused to just a few mils diameter (by mirror 19) in the region of the modulator it can be located conveniently with thermofax paper. Thermofax paper turns black in three seconds at about 1 watt/sq cm.

The active acoustic volume of the Bragg modulator is about 1 cm long (along the laser beam), about 1 mm wide, perpendicular to the laser beam and perpendicular to the acoustic beam, and of course, extends the full length of the window in the direction of the acoustic beam propagation. Optimum operation requires centering the laser beam in this active volume and arranging the angle of incidence between the laser beam and the acoustic wavefronts to be 77/2 milliradians. The unused, undeflected signal can be absorbed in a piece of carbon block or asbestos. It is of course very important that rated levels not be exceeded on the detector (about 1 milliwatt) or on the Bragg modulator (about 100 w/cm^2 over small areas).

The gratings, 15 and 23, must be aligned on the same transition, preferably P-20, with a grating spectrometer.

Final adjustment of the TEA laser cavity is accomplished by observing the symmetry of energy distribution pattern on a carbon block. Transverse modes will be observed as multiple heterodyne beat frequencies of a few MHz from the longitudinal mode.


DATE:
ILME